Microscopics of disordered two-dimensional electron gases under high magnetic fields: Equilibrium properties and dissipation in the hydrodynamic regime

Thierry Champel,[1] Serge Florens,[2] and Léonie Canet[1]

[1]*Laboratoire de Physique et Modélisation des Milieux Condensés, CNRS and Université Joseph Fourier, B.P. 166,
25 Avenue des Martyrs, 38042 Grenoble Cedex 9, France*

[2]*Institut Néel, CNRS and Université Joseph Fourier, B.P. 166, 25 Avenue des Martyrs, 38042 Grenoble Cedex 9, France*

We develop in detail a formalism [as a sequel to the work of T. Champel and S. Florens, Phys. Rev. B **75**, 245326 (2007)] that is well suited for treating quantum problems involving slowly varying potentials at high magnetic fields in two-dimensional electron gases. For an arbitrary smooth potential we show that electronic Green's function is fully determined by closed recursive expressions that take the form of a high magnetic-field expansion in powers of the magnetic length l_B. For illustration we determine entirely Green's function at order l_B^3, which is then used to obtain quantum expressions for the local charge and current electronic densities at equilibrium. Such results are valid at high but finite magnetic fields and for arbitrary temperatures, as they take into account Landau level mixing processes and wave-function broadening. We also check the accuracy of our general functionals against the exact solution of a one-dimensional parabolic confining potential, demonstrating the controlled character of the theory to get equilibrium properties. Finally, we show that transport in high magnetic fields can be described hydrodynamically by a local equilibrium regime and that dissipation mechanisms and quantum tunneling processes are intrinsically included at the microscopic level in our high magnetic-field theory. We calculate microscopic expressions for the local conductivity tensor, which possesses both transverse and longitudinal components, providing a microscopic basis for the understanding of dissipative features in quantum Hall systems.

I. INTRODUCTION

A. General motivation

Almost 30 years after the discovery of the quantum Hall effect,[1,2] two-dimensional electron gases under magnetic fields continue to attract a considerable interest both experimentally and theoretically and have revealed a rich world of surprising physics. Newly discovered features concern, e.g., the zero resistance states under microwave illumination[3] and the peculiar Landau-level quantization in graphene.[4] Concerning the integer quantum Hall effect (IQHE) itself, direct local imaging techniques[5–8] have revealed new electron-electron correlation phenomena and allowed a finer understanding of the microscopic ingredients at work.

On the theoretical side, the quantization of the Hall resistance observed in the IQHE relies on the understanding of the quantum motion of charged particles in a two-dimensional disordered electrostatic landscape in the presence of a strong perpendicular magnetic field.[9–18] As the main effects of the electron-electron interaction can be taken into account in the integer regime at the single-particle level, using a Hartree approach to screening,[19,20] the calculation of equilibrium properties, such as the local electronic density and the distribution of permanent currents throughout the sample, can be carried out from a one-particle random Schrödinger equation. The precise resolution of this problem constitutes the first and important step toward a microscopic description that underlies the more complex nonequilibrium phenomena of the quantum Hall effect in its generality.

Despite the overall good understanding gained after several decades of research,[10,12–25] a simple and general microscopic approach for the physics of quantum Hall systems is surprisingly still lacking. Computer-based simulations have been proposed,[26,27] but rely on heavy numerics in the case of two-dimensional disordered potentials, and are not well suited for the computation of out-of-equilibrium properties. Even in the linear-response regime, they are certainly unable to address minute aspects such as the tiny deviations to the Hall resistance quantization. Analytical approaches are better adapted to formulate out-of-equilibrium calculations but face the need to reliably handle in a self-consistent screening theory both the formation of Landau energy levels at quantizing magnetic fields and the complexity of the random potential.

At present, the theory of the integer quantum Hall effect relies on two main cornerstones, which do await a unified description. On the one hand, equilibrium density profiles are generally computed within a semiclassical Thomas-Fermi approach,[19,20,28,29] leading to a description of the quantum Hall liquid in terms of compressible and incompressible regions. These calculations have however proved to be only qualitatively accurate[30] and fail at low temperature, where quantum broadening due to the electronic wave function becomes important. Transport properties are on the other hand conveniently formulated in the Büttiker edge state formalism,[19,24,28] which nevertheless needs input from more microscopic calculations of the bulk properties. This scattering theory becomes also very cumbersome to describe dissipative features of macroscopic samples. An alternative successful semiclassical approach to transport[29–33] assumes local Ohm's law at a phenomenological level. A simple and controlled quantum approach to both equilibrium and out-of-equilibrium properties of quantum Hall fluids is thus clearly needed.

B. Review of the high magnetic-field approaches: The semiclassical limit

A popular approach to the IQHE is the high magnetic-field limit, in which case the center-of-mass motion of the electron becomes essentially classical. A quantum description is only kept for the orbital effects associated with the Landau-level formation.[10,12–15] The basic physical idea behind these works is that the effective potential seen by the electrons in quantum Hall systems is quite smooth at the scale of the magnetic length $l_B = \sqrt{\hbar c / |e| B}$ (here $\hbar$ is Planck's constant divided by 2π, c is the velocity of light, B is the magnetic-field strength, and $|e|$ is the absolute value of the electric charge). This permits a simple mathematical treatment of the Schrödinger equation using as a small parameter the ratio of the magnetic length to the typical correlation length of the random potential. This point of view is certainly vindicated experimentally by the fact that the impurities in semiconducting heterostructures are located outside the two-dimensional layer of conduction electrons, while l_B is an extremely small length scale which falls below 10 nm for magnetic fields above 5 T. It is tempting to believe that all aspects of the quantum Hall effect should be captured accurately in this limit.

While the idea is certainly not new, it is interesting to note that no fully quantum treatment of the high-field regime is currently available, which is the issue we want to address in this paper. Focusing first on the semiclassical corrections to the $B = \infty$ limit, it is known that systematic calculations are quite cumbersome, even at the lowest orders in the l_B expansion, due to the Landau level mixing,[13,34] so that new tools are certainly needed. A first technical step in this direction was made by two of us in a recent publication[35] by introducing well-suited coherent state Green's functions. These so-called vortex states with the quantum numbers $\nu = (m, \mathbf{R})$, where m is the Landau-level index and $\mathbf{R}$ the position of a localized vortexlike wave function, form an overcomplete basis of eigenfunctions with no preferred symmetry, in contrast to the widely used translation-invariant Landau states or the rotation-invariant circular states. They thus permit a great adaptability to the spatial variations of the local electric fields, coming from either random impurity donors, confinement potentials due to external gates, or macroscopic voltage drops. This formulation also allows one to classify Landau level mixing processes in a simple and natural manner, an important point for the investigation of quantum transport properties, as the matrix elements of the current density necessarily relate adjacent Landau levels.

Our first implementation of this technique[35] has demonstrated, not surprisingly, that the usual semiclassical approach to the quantum Hall effect (limited to spectral properties) could be easily recovered by a straightforward expansion of vortex Green's function in powers of the magnetic length. In this view, the vortex state coordinate $\mathbf{R}$ can be identified in the limit $l_B \to 0$ with the slow classical center-of-mass drifting motion, which completely decouples from the faster cyclotron motion.

C. Toward a unified quantum description at high magnetic field

The present paper has two aims. First, we want to provide an accurate quantum treatment of the local equilibrium properties of quantum Hall systems. For this purpose, we offer simple functionals of the arbitrary local electrostatic potential that describe both the local charge and current densities. These results may have important bearings for microscopic modelizations of real devices based on Hartree-Fock or more refined local density approximation (LDA) calculations, as they avoid the numerical costs in solving the random Schrödinger equation in a magnetic field. The knowledge of the current density functional can be used in a second step to obtain out of equilibrium transport equations, which take a simple hydrodynamic form at high magnetic fields. This step allows us to derive microscopically a simple and local expression for the conductivity tensor. We show that in contrast to the well-known drift contribution to the transverse Hall conductivity,[36] dissipative longitudinal components first appear at order l_B^2. These contributions had not been obtained previously in the literature to our knowledge. This method also allows one in principle to derive microscopically the dominant nonlocal corrections to local Ohm's law. A general understanding of the dissipative features in the integer regime seems now possible at the microscopic level.

D. Organization of the paper

Because the paper involves several technical developments, we hereafter guide the reader through the main results obtained. Section II is used to introduce vortex Green's functions and reformulate in a more systematic manner the results obtained in Ref. 35. Two important formulas are found that determine completely Green's functions both in the vortex coordinates [Eq. (26)] and in the electronic coordinates [Eq. (44)]. These are the starting point for the computation of all physical observables. The local electronic charge density is thus derived up to order l_B^2 in Sec. III and is given by formulas (50), (56), and (58). We emphasize beforehand that all these expressions take into account quantum smearing effects from the wave function and extend the semiclassical results (also derived in this section) to much lower temperatures. Similarly, the (equilibrium) local electronic current density is computed to the same order in Sec. IV and is given by Eqs. (72), (75), (C6), (C8), and (C10). Again, the semiclassical current density can be obtained from these expressions and is given by Eqs. (73), (76), and (C11)–(C14). We then provide in Sec. V two important checks of our theory against an exactly solvable model of a one-dimensional parabolic confinement potential. First, the analytic semiclassical formulas for the local observables obtained in Secs. III and IV are compared with the strict expansion in l_B from the exact model and shown to match precisely, strengthening the mathematical foundation of our theory. Second, a more quantitative comparison is made between the quantum expressions obtained for the electronic density in Sec. III and the exact results at finite values of the magnetic length. This shows that the expansion proposed here is converging quite rapidly, even for a confining potential that is not exceedingly smooth. Because the vortex states do not favor any special symmetric situation, similar quantitative results should be obtained for an arbitrary two-dimensional smooth disordered potential. In the limit of zero temperature, this comparison

also shows the need for a resummation of the quantum expressions to infinite order in l_B, modifying both the vortex wave functions and energies and allowing a possible connection to the edge state picture. Finally, Sec. VI investigates nonequilibrium properties in the integer quantum Hall regime and provides a microscopic derivation of the local conductivity tensor in the semiclassical regime [formula (108)]. The origin of dissipation is discussed, and a general conclusion showing future directions of our work closes the paper. Some extra technical details are given in several appendixes.

II. HIGH FIELD EXPANSION WITHIN THE VORTEX STATES REPRESENTATION

A. Vortex states

The vortex states under which our quantum high magnetic-field theory reposes are eigenstates of the free Hamiltonian,

$$H_0 = \frac{1}{2m^*}\left(-i\hbar\boldsymbol{\nabla}_\mathbf{r} - \frac{e}{c}\mathbf{A}(\mathbf{r})\right)^2, \tag{1}$$

describing a single electron of effective mass m^* and of charge $e = -|e|$ confined in a (xy) two-dimensional plane under a perpendicular magnetic field $\mathbf{B}$ (pointing in the z direction). In the symmetrical gauge,

$$\mathbf{A}(\mathbf{r}) = \frac{\hbar c}{|e|}\frac{1}{2l_B^2}\begin{pmatrix} -y \\ x \end{pmatrix},$$

the vortex wave functions, with quantum number $\nu = (m, \mathbf{R})$, are written in terms of the electronic variables $\mathbf{r}$ as[11,35]

$$\Psi_{m,\mathbf{R}}(\mathbf{r}) = \frac{1}{\sqrt{2\pi m!}\,l_B}\left(\frac{x - X + i(y - Y)}{\sqrt{2}l_B}\right)^m$$
$$\times \exp\left[-\frac{(x-X)^2 + (y-Y)^2 + 2i(yX - xY)}{4l_B^2}\right]. \tag{2}$$

The associated energy levels read

$$E_{m,\mathbf{R}} = (m + 1/2)\hbar\omega_c \equiv E_m, \tag{3}$$

where $\omega_c = |e|B/m^*c$ is the cyclotron pulsation. The energy levels are independent of the position $\mathbf{R}$, and their quantization is uniquely related to the (topological) quantization of the circulation of any paths enclosing the position $\mathbf{r} = \mathbf{R}$ which corresponds to a phase singularity of the wave function $\Psi_{m,\mathbf{R}}(\mathbf{r})$ (note that this wave function vanishes only at the point $\mathbf{r} = \mathbf{R}$ where its phase is ill-defined: it describes a vortex).

As is clear from Eq. (3) the Landau energy levels are highly degenerate, so that there is a great freedom in the choice of a basis of states. However, a judicious choice for the set of quantum numbers appears essential when considering perturbations that lift this huge energy degeneracy. A peculiarity of the vortex states, which could appear at the first glance as a drawback, is that they are nonorthogonal with respect to the degeneracy quantum number $\mathbf{R}$. Indeed, the overlap between two vortex states is given by

$$\langle \nu_1 | \nu_2 \rangle = \delta_{m_1, m_2}\langle \mathbf{R}_1 | \mathbf{R}_2 \rangle, \tag{4}$$

$$\langle \mathbf{R}_1 | \mathbf{R}_2 \rangle = \exp\left[-\frac{(\mathbf{R}_1 - \mathbf{R}_2)^2 - 2i\hat{\mathbf{z}} \cdot (\mathbf{R}_1 \times \mathbf{R}_2)}{4l_B^2}\right], \tag{5}$$

where $\hat{\mathbf{z}}$ is the unit vector along the perpendicular magnetic field.

On the contrary, the other well-known eigenstates of H_0, the Landau and circular basis states, which are commonly used for quantum calculations, are orthogonal. But since they are highly symmetric states, they lead to unsolved technical difficulties when considering a random potential in high magnetic fields, which mixes in a very complicated way the two quantum numbers. The vortex basis, which has no intrinsic symmetry (the nonorthogonality of the vortex states arises from this property), allows one to overcome this drawback. The possibility[35] to work with this basis is, in fact, provided by the coherent character of the vortex position degree of freedom (the algebra obeyed by the degeneracy quantum number $\mathbf{R}$ is that of coherent states).

B. Dyson equation in the vortex representation

From now on and throughout the paper, we consider that the Hamiltonian contains in addition to the kinetic part H_0 a potential-energy term $V(\mathbf{r})$, which we let completely unspecified

$$H = H_0 + V(x, y). \tag{6}$$

The Dyson equation written within the vortex representation $|\nu\rangle = |m, \mathbf{R}\rangle$ then takes the form[35]

$$(\omega - E_{m_1} \pm i\delta)G_{\nu_1;\nu_2}^{R,A}(\omega) = \langle \nu_1 | \nu_2 \rangle + \sum_{\nu_3} V_{\nu_1;\nu_3}G_{\nu_3;\nu_2}^{R,A}(\omega), \tag{7}$$

where $G_{\nu_1;\nu_2}^{R,A}(\omega)$ are retarded and advanced Green's functions connecting two vortex states ν_1 and ν_2 (in the energy representation). The sum over the vortex quantum numbers ν appearing into the Dyson equation stands for

$$\sum_\nu = \sum_{m=0}^{+\infty}\int \frac{d\mathbf{R}}{2\pi l_B^2}. \tag{8}$$

The matrix elements of the potential $V(\mathbf{r})$ in the vortex basis are given by

$$V_{\nu_1;\nu_2} = \int d^2\mathbf{r}\, V(\mathbf{r})\Psi_{m_1,\mathbf{R}_1}^*(\mathbf{r})\Psi_{m_2,\mathbf{R}_2}(\mathbf{r}) = \langle \mathbf{R}_1 | \mathbf{R}_2 \rangle v_{\nu_1;\nu_2} \tag{9}$$

where, for a practical purpose which will appear obvious in the following, the overlap between the two vortex states has been extracted. Similarly for retarded and advanced Green's function, we extract the vortex overlap,

$$G_{\nu_1;\nu_2}^{R,A}(\omega) = \langle \mathbf{R}_1 | \mathbf{R}_2 \rangle g_{\nu_1;\nu_2}^{R,A}, \tag{10}$$

where the dependence on frequency ω is not explicited anymore in order not to burden the expressions. Substituting

expressions (9) and (10) in Eq. (7), we get a Dyson equation for the function $g_{\nu_1;\nu_2}^{R,A}$ which reads

$$(\omega - E_{m_1} \pm i\delta)g_{\nu_1;\nu_2}^{R,A} = \delta_{m_1,m_2} + \sum_{\nu_3} v_{\nu_1;\nu_3}g_{\nu_3;\nu_2}^{R,A}$$

$$\times \frac{\langle \mathbf{R}_1|\mathbf{R}_3\rangle\langle \mathbf{R}_3|\mathbf{R}_2\rangle}{\langle \mathbf{R}_1|\mathbf{R}_2\rangle}, \qquad (11)$$

where

$$\frac{\langle \mathbf{R}_1|\mathbf{R}_3\rangle\langle \mathbf{R}_3|\mathbf{R}_2\rangle}{\langle \mathbf{R}_1|\mathbf{R}_2\rangle} = \exp\left\{-\frac{[\mathbf{R}_3 - (\mathbf{c}_{12} + i\mathbf{d}_{12} \times \hat{\mathbf{z}})]^2}{2l_B^2}\right\}. \qquad (12)$$

We have introduced here the center-of-mass coordinates $\mathbf{c}_{12} = (\mathbf{R}_1 + \mathbf{R}_2)/2$ and the relative coordinates $\mathbf{d}_{12} = (\mathbf{R}_2 - \mathbf{R}_1)/2$.

Provided that $V(x,y)$ is an analytic function of both x and y, the reduced matrix element $v_{\nu_1;\nu_2}$ of the potential appearing in Eq. (9) can be written[35] as a series in powers of the magnetic length l_B,

$$v_{\nu_1;\nu_2} = \sum_{j=0}^{+\infty} \left(\frac{l_B}{\sqrt{2}}\right)^j v_{\nu_1;\nu_2}^{(j)}, \qquad (13)$$

$$v_{\nu_1;\nu_2}^{(j)} = \sum_{k=0}^{j} \frac{(m_1+k)!}{\sqrt{m_1!\,m_2!}} \frac{\delta_{m_1+k,m_2+j-k}}{k!\,(j-k)!}(\partial_X + i\partial_Y)^k$$

$$\times (\partial_X - i\partial_Y)^{j-k}V(\mathbf{R})|_{\mathbf{c}_{12}+i\mathbf{d}_{12}\times\hat{\mathbf{z}}}. \qquad (14)$$

Solving exactly Dyson equation [Eq. (11)] for an arbitrary potential V is certainly a formidable task. Remarkably, however, from the structure of this equation, one can show that the function $g_{\nu_1;\nu_2}$ depends on the two vortex coordinates $\mathbf{R}_1$ and $\mathbf{R}_2$ through the special combination $\mathbf{c}_{12} + i\mathbf{d}_{12} \times \hat{\mathbf{z}}$ only. Indeed, let us differentiate Eq. (11) with respect to the first vortex position,

$$(\omega - E_{m_1} \pm i\delta)(\partial_{X_1} - i\partial_{Y_1})g_{\nu_1;\nu_2}^{R,A} = \sum_{\nu_3} (\partial_{X_1} - i\partial_{Y_1})$$

$$\times \left\{v_{\nu_1;\nu_3}g_{\nu_3;\nu_2}^{R,A}\frac{\langle \mathbf{R}_1|\mathbf{R}_3\rangle\langle \mathbf{R}_3|\mathbf{R}_2\rangle}{\langle \mathbf{R}_1|\mathbf{R}_2\rangle}\right\}. \qquad (15)$$

Then, noting that from Eqs. (12) and (14),

$$(\partial_{X_1} - i\partial_{Y_1})\left\{\frac{\langle \mathbf{R}_1|\mathbf{R}_3\rangle\langle \mathbf{R}_3|\mathbf{R}_2\rangle}{\langle \mathbf{R}_1|\mathbf{R}_2\rangle}\right\} = 0, \qquad (16)$$

$$(\partial_{X_1} - i\partial_{Y_1})v_{\nu_1;\nu_3} = 0, \qquad (17)$$

and considering Eq. (15), we arrive to the relation

$$\partial_{X_1}g_{\nu_1;\nu_2}^{R,A} = i\partial_{Y_1}g_{\nu_1;\nu_2}^{R,A}. \qquad (18)$$

We can establish similarly from the other Dyson equation (i.e., $G = G_0 + GVG_0$) that

$$\partial_{X_2}g_{\nu_1;\nu_2}^{R,A} = -i\partial_{Y_2}g_{\nu_1;\nu_2}^{R,A}. \qquad (19)$$

We thus deduce from these two relations [Eqs. (18) and (19)] that the function g depends on the vortex positions $\mathbf{R}_1$ and $\mathbf{R}_2$ in the following way:

$$g_{\nu_1;\nu_2} = g_{m_1;m_2}\left(\frac{\mathbf{R}_1 + \mathbf{R}_2 + i(\mathbf{R}_2 - \mathbf{R}_1) \times \hat{\mathbf{z}}}{2}\right). \qquad (20)$$

This exact result implies that vortex Green's functions will be entirely determined once the function $g_{\nu_1;\nu_2}$ at coinciding vortex positions $\mathbf{R}_1 = \mathbf{R}_2 \equiv \mathbf{R}$ are known (provided it is analytic in the complex plane). This task is addressed in Sec. II C.

C. High magnetic-field expansion of vortex Green's function

We are mainly interested in the high magnetic-field regime, i.e., when the magnetic length $l_B = \sqrt{\hbar c/|e|B}$ is small compared to the typical length scale of the (possibly random) potential $V(\mathbf{r})$. We aim at solving the Dyson equation [Eq. (11)] as a systematic expansion in powers of l_B, i.e., expanding the function $g_{\nu_1;\nu_2}$ as

$$g_{\nu_1;\nu_2} = \sum_{j=0}^{+\infty} \left(\frac{l_B}{\sqrt{2}}\right)^j g_{\nu_1;\nu_2}^{(j)}. \qquad (21)$$

This expansion is possible because, using the change in function (10), the nonanalytic dependence on the magnetic length l_B which was contained in the first term of the right-hand side (rhs) of Eq. (7) has been fully transferred to the overlap terms [Eq. (12)] appearing in the integral contribution of the Dyson equation [Eq. (11)]. At large magnetic fields (i.e., small l_B) and when $\mathbf{R}_1$ is close to $\mathbf{R}_2$ the main contribution to the integral over $\mathbf{R}_3$ in Eq. (11) comes when $\mathbf{R}_3$ is near both positions $\mathbf{R}_1$ and $\mathbf{R}_2$. Because Green's function (20) depends on a linear combination of the two vortex locations, it is enough to calculate vortex Green's function at coinciding points $\mathbf{R}_1 = \mathbf{R}_2 \equiv \mathbf{R}$, so that, from Eq. (11), only the value of the function $v_{m_1,\mathbf{R};m_3,\mathbf{R}_3}g_{m_3,\mathbf{R}_3;m_2,\mathbf{R}}$ has to be considered. The Dyson equation can now be solved by expanding the nonlocal functions g and v around coinciding points using a Taylor series at $\mathbf{R}_3$ close to $\mathbf{R}$,

$$g_{m_3,\mathbf{R}_3;m_2,\mathbf{R}} = \sum_{k=0}^{+\infty} \frac{[(X_3 - X) - i(Y_3 - Y)]^k}{k!\,2^k}(\partial_X + i\partial_Y)^k g_{m_3;m_2}(\mathbf{R}), \qquad (22)$$

$$v_{m_1,\mathbf{R};m_3,\mathbf{R}_3} = \sum_{k'=0}^{+\infty} \frac{[(X_3 - X) + i(Y_3 - Y)]^{k'}}{k'!\,2^{k'}}(\partial_X - i\partial_Y)^{k'} v_{m_1;m_3}(\mathbf{R}), \qquad (23)$$

where we have taken into account the spatial dependences of v [see Eq. (14)] and g [see Eq. (20)]. The integral over the vortex position $\mathbf{R}_3$ in Eq. (11) can then be evaluated using the following property of Gaussian integrals:

$$\int \frac{d^2\mathbf{R}_3}{2\pi l_B^2} v_{m_1,\mathbf{R};m_3,\mathbf{R}_3} g_{m_3,\mathbf{R}_3;m_2,\mathbf{R}} e^{-(\mathbf{R}_3-\mathbf{R})^2/2l_B^2}$$

$$= \int \frac{d^2\mathbf{R}_3}{2\pi l_B^2} \sum_{k,k'=0}^{+\infty} [(X_3-X)-i(Y_3-Y)]^k [(X_3-X)$$

$$+ i(Y_3-Y)]^{k'} \times \frac{e^{-(\mathbf{R}_3-\mathbf{R})^2/2l_B^2}}{k!\,k'!\,2^{k+k'}} (\partial_X - i\partial_Y)^{k'} v_{m_1;m_3}(\mathbf{R})$$

$$\times (\partial_X + i\partial_Y)^k g_{m_3;m_2}(\mathbf{R}), \tag{24}$$

$$= \sum_{k=0}^{+\infty} \left(\frac{l_B}{\sqrt{2}}\right)^{2k} \frac{1}{k!} (\partial_X - i\partial_Y)^k v_{m_1;m_3}(\mathbf{R}) (\partial_X + i\partial_Y)^k g_{m_3;m_2}(\mathbf{R}). \tag{25}$$

Combining the different series expansions of the matrix elements of the potential [Eqs. (13) and (14)] of vortex Green's function $g^{R,A}$ [Eq. (21)] and of the integral term [Eq. (25)] in the Dyson equation, the functions $g_{\nu_1;\nu_2}^{R,A}$ at coinciding points $\mathbf{R}_1 = \mathbf{R}_2$ are then entirely determined order by order in powers of the magnetic length l_B. In fact, vortex Green's function $g^{(n)}$ at order l_B^n is related to the terms $g^{(l)}$ (with $l < n$) through *a closed-form recursive relation*,

$$g_{m_1;m_2}^{(n)}(\mathbf{R}) = g_{m_1;m_1}^{(0)}(\mathbf{R}) \sum_{l=0}^{n-1} \sum_{j=0}^{n-l} \sum_{k=0}^{(n-l)/2} \frac{1}{k!} \delta_{n,2k+j+l} \sum_{m_3=m_1-j}^{m_1+j}$$

$$\times (\partial_X + i\partial_Y)^k g_{m_3;m_2}^{(l)}(\mathbf{R}) (\partial_X - i\partial_Y)^k v_{m_1;m_3}^{(j)}(\mathbf{R}), \tag{26}$$

where the function $v^{(j)}$ is given by Eq. (14) at coinciding points,

$$v_{m_1;m_2}^{(j)}(\mathbf{R}) = \sum_{k=0}^{j} \frac{(m_1+k)!}{\sqrt{m_1!\,m_2!}} \frac{\delta_{m_1+k,m_2+j-k}}{k!\,(j-k)!} (\partial_X + i\partial_Y)^k$$

$$\times (\partial_X - i\partial_Y)^{j-k} V(\mathbf{R}), \tag{27}$$

and the zeroth order contribution $g^{(0)}$, which suffices to determine the whole series, is given in Eq. (29) below.

Obviously, the present method generates a *systematic* expansion for vortex Green's functions in series of the magnetic length l_B. Even for a disordered potential that is smooth on the scale of l_B, the question of the accuracy and convergence of this expansion has to be addressed. We refer the reader both to a general discussion of this important point in Sec. II F and to a concrete comparison with an exactly solvable model in Sec. V.

D. Vortex Green's functions up to order l_B^3

For the calculations to follow in the rest of the paper, vortex Green's functions up to order l_B^3 will be needed, and these useful expressions are given here. At leading order (zeroth order in magnetic length) the equation determining the function $g^{(0)}$ is trivially found by setting $k=0$ in formula (25), which is then reported in Dyson equation [Eq. (11)],

$$(\omega - E_{m_1} \pm i\delta) g_{m_1;m_2}^{(0)}(\mathbf{R}) = \delta_{m_1,m_2} + V(\mathbf{R}) g_{m_1;m_2}^{(0)}(\mathbf{R}). \tag{28}$$

This equation is entirely closed and yields straightforwardly,

$$g_{m_1;m_2}^{(0)R,A}(\mathbf{R}) = \frac{\delta_{m_1,m_2}}{\omega - \xi_{m_1}(\mathbf{R}) \pm i\delta}, \tag{29}$$

with $\xi_m(\mathbf{R}) = E_m + V(\mathbf{R})$. Green's function at leading order is diagonal with respect to the vortex circulation quantum number m. We regard this robustness of m independently of the detailed form and strength of the potential V as a signature of its topological nature. We see that, in addition to a kinetic term (E_m), the energy of the vortex state $\xi_m(\mathbf{R})$ now also contains the value of the potential energy $V(\mathbf{R})$ at the vortex location, which lifts the huge degeneracy of the Landau levels. This leading order of the calculation clearly corresponds to the strict semiclassical limit[10,11,13,34] at $l_B = 0$.

All subleading contributions are straightforwardly determined using the recursive relation (26), which for $n=1$ gives the order l_B contribution,

$$g_{m_1;m_2}^{(1)R,A}(\mathbf{R}) = g_{m_1;m_1}^{(0)}(\mathbf{R}) g_{m_2;m_2}^{(0)}(\mathbf{R}) v_{m_1;m_2}^{(1)}(\mathbf{R}), \tag{30}$$

$$= \frac{v_{m_1;m_2}^{(1)}(\mathbf{R})}{[\omega - \xi_{m_1}(\mathbf{R}) \pm i\delta][\omega - \xi_{m_2}(\mathbf{R}) \pm i\delta]}, \tag{31}$$

where from Eq. (14)

$$v_{m_1;m_2}^{(1)}(\mathbf{R}) = [\sqrt{m_2}\,\delta_{m_1+1,m_2}(\partial_X + i\partial_Y) + \sqrt{m_1}\,\delta_{m_1,m_2+1}$$

$$\times (\partial_X - i\partial_Y)] V(\mathbf{R}). \tag{32}$$

We thus see that a mixing between adjacent Landau levels appears in the presence of a gradient of the potential V.

For the determination of the function $g^{(2)}$, the matrix elements of the potential at order l_B^2 are needed, which read from Eq. (14),

$$v_{m_1;m_2}^{(2)}(\mathbf{R}) = \frac{1}{2} \frac{\max(m_1,m_2)!}{\sqrt{m_1!\,m_2!}} [\delta_{m_1+2,m_2}(\partial_X + i\partial_Y)^2 + \delta_{m_1,m_2+2}$$

$$\times (\partial_X - i\partial_Y)^2 + 2(m_1+1)\delta_{m_1,m_2}\Delta_{\mathbf{R}}] V(\mathbf{R}). \tag{33}$$

Recursion relation (26) at this order gives

$$g_{m_1;m_2}^{(2)}(\mathbf{R}) = g_{m_1;m_1}^{(0)} \left[v_{m_1;m_2}^{(2)}(\mathbf{R}) g_{m_2;m_2}^{(0)}(\mathbf{R}) + \sum_{m_3} v_{m_1;m_3}^{(1)}(\mathbf{R}) \right.$$

$$\left. \times g_{m_3;m_2}^{(1)}(\mathbf{R}) + \delta_{m_1,m_2} \boldsymbol{\nabla}_{\mathbf{R}} V(\mathbf{R}) \cdot \boldsymbol{\nabla}_{\mathbf{R}} g_{m_1;m_1}^{(0)}(\mathbf{R}) \right]. \tag{34}$$

The function $g^{(2)}$ consequently contains diagonal elements ($m_1 = m_2$) and elements mixing Landau levels separated by an energy of $2\hbar\omega_c$ (terms with $m_1 = m_2 \pm 2$),

$$g^{(2)}_{m_1;m_2}(\mathbf{R}) = \delta_{m_1,m_2}\left[(m_1+1)\frac{\Delta_{\mathbf{R}}V}{\omega^2_{m_1}} + \left(\frac{m_1+1}{\omega_{m_1+1}} + \frac{m_1}{\omega_{m_1-1}} + \frac{1}{\omega_{m_1}}\right)\frac{|\nabla_{\mathbf{R}}V|^2}{\omega^2_{m_1}}\right] + \sqrt{m_1+1}\sqrt{m_1+2}\,\delta_{m_1+2,m_2}$$

$$\times \left[\frac{(\partial_X + i\partial_Y)^2 V}{2\omega_{m_1}\omega_{m_2}} + \frac{[(\partial_X + i\partial_Y)V]^2}{\omega_{m_1}\omega_{m_1+1}\omega_{m_1+2}}\right] + \sqrt{m_2+1}\sqrt{m_2+2}\,\delta_{m_1,m_2+2}\left[\frac{(\partial_X - i\partial_Y)^2 V}{2\omega_{m_1}\omega_{m_2}} + \frac{[(\partial_X - i\partial_Y)V]^2}{\omega_{m_2+2}\omega_{m_2+1}\omega_{m_2}}\right], \qquad (35)$$

where we have introduced the short-hand notation $\omega_m = \omega - \xi_m(\mathbf{R}) \pm i\delta$.

As for third-order Green's function, we shall not write here the full expression, which is rather cumbersome. The derivation of these terms from Eq. (26) is however straightforward, and Appendix A provides the components that are needed for subsequent calculations.

E. Green's functions in the electronic representation

The aim of this section is to connect local vortex Green's function, determined previously in the magnetic length expansion, to physical observables. For this purpose, we need to express Green's functions in terms of the electronic positions $\mathbf{r}$, which, thanks to the completeness relation satisfied by the vortex states,[35] can be obtained as

$$G(\mathbf{r},\mathbf{r}',\omega) = \sum_{\nu_1,\nu_2} G_{\nu_1;\nu_2}(\omega)\Psi^*_{\nu_2}(\mathbf{r}')\Psi_{\nu_1}(\mathbf{r}). \qquad (36)$$

Rewriting in terms of the vortex location $\mathbf{R}$ and circulation m, this expression reads

$$G(\mathbf{r},\mathbf{r}',\omega) = \int\frac{d^2\mathbf{R}_1}{2\pi l^2_B}\int\frac{d^2\mathbf{R}_2}{2\pi l^2_B}\sum_{m_1,m_2}G_{m_1,\mathbf{R}_1;m_2,\mathbf{R}_2}(\omega)$$

$$\times \Psi^*_{m_2,\mathbf{R}_2}(\mathbf{r}')\Psi_{m_1,\mathbf{R}_1}(\mathbf{r}). \qquad (37)$$

Besides the double integral in the above formula, the difficulty we immediately encounter is that nonlocal vortex Green's function is in principle needed. Again, we are going to see that key formula (20) allows us to reformulate this expression in terms of local vortex Green's function determined in Sec. II C. Inserting expression (10), we first write the different exponential factors appearing into the integrand of expression (37) as

$$\langle\mathbf{R}_1|\mathbf{R}_2\rangle e^{-[(\mathbf{r}-\mathbf{R}_1)^2 - 2i(\mathbf{r}\times\mathbf{R}_1)\cdot\hat{\mathbf{z}}]/4l^2_B}e^{-[(\mathbf{r}'-\mathbf{R}_2)^2 + 2i(\mathbf{r}'\times\mathbf{R}_2)\cdot\hat{\mathbf{z}}]/4l^2_B}$$

$$= e^{-2\mathbf{d}^2_{12}/l^2_B}e^{-[(\mathbf{r}-\mathbf{R})^2 - 2i(\mathbf{r}\times\mathbf{R})\cdot\hat{\mathbf{z}}]/4l^2_B}e^{-[(\mathbf{r}'-\mathbf{R})^2 + 2i(\mathbf{r}'\times\mathbf{R})\cdot\hat{\mathbf{z}}]/4l^2_B}, \qquad (38)$$

where $\mathbf{R} = \mathbf{c}_{12} - i\mathbf{d}_{12}\times\hat{\mathbf{z}}$ is a complex combination of the center of mass and of the relative vortex coordinates. Similarly, the polynomial parts of the vortex wave functions can be written as

$$[x' - X_2 - i(y'-Y_2)]^{m_2}[x - X_1 + i(y-Y_1)]^{m_1}$$

$$= [x' - X - i(y'-Y)]^{m_2}[x - X + i(y-Y)]^{m_1}. \qquad (39)$$

It thus seems natural to introduce the change in variables

$(\mathbf{R}_1,\mathbf{R}_2)\to(\mathbf{R},\mathbf{d}_{12})$. The variables X and Y lie *a priori* on lines in the complex plane as a result of the complex shift $(-i\mathbf{d}_{12}\times\hat{\mathbf{z}})$. Using the analycity property of the functions in the integrand, the contours of integration can be deformed to the real axes. The dependences on the variables $\mathbf{R}$ and $\mathbf{d}_{12}$ in the function $g_{m_1,\mathbf{R}_1;m_2,\mathbf{R}_2}$ are made separable using Eq. (20) and expanding the nonlocal g function as

$$g_{m_1,\mathbf{R}_1;m_2,\mathbf{R}_2} = g_{m_1;m_2}(\mathbf{c}_{12} + i\mathbf{d}_{12}\times\hat{\mathbf{z}}), \qquad (40)$$

$$= g_{m_1;m_2}(\mathbf{R} + 2i\mathbf{d}_{12}\times\hat{\mathbf{z}}), \qquad (41)$$

$$= \sum_{j=0}^{+\infty}\frac{[2i(\mathbf{d}_{12}\times\hat{\mathbf{z}})\cdot\nabla_{\mathbf{R}}]^j}{j!}g_{m_1;m_2}(\mathbf{R}), \qquad (42)$$

$$= \sum_{j=0}^{+\infty}\sum_{k=0}^{j}\frac{(d_{12x} - id_{12y})^k(d_{12x} + id_{12y})^{j-k}}{k!\,(j-k)!\,(-1)^k}$$

$$\times (\partial_X + i\partial_Y)^k(\partial_X - i\partial_Y)^{j-k}g_{m_1;m_2}(\mathbf{R}), \qquad (43)$$

where we have used $2i(\mathbf{d}_{12}\times\hat{\mathbf{z}})\cdot\nabla_{\mathbf{R}} = (d_{12x} + id_{12y})(\partial_X + i\partial_Y) - (d_{12x} - id_{12y})(\partial_X - i\partial_Y)$ and then applied the binomial theorem. Inserting expansion (43) into Eq. (37) and using Eqs. (38) and (39), we can then perform the integral over the relative coordinates $\mathbf{d}_{12}$ to finally obtain

$$G(\mathbf{r},\mathbf{r}',\omega) = \int\frac{d^2\mathbf{R}}{2\pi l^2_B}\sum_{m,m'}\Psi^*_{m',\mathbf{R}}(\mathbf{r}')\Psi_{m,\mathbf{R}}(\mathbf{r})$$

$$\times \sum_{k=0}^{+\infty}\frac{1}{k!}\left(-\frac{l^2_B}{2}\Delta_{\mathbf{R}}\right)^k g_{m;m'}(\mathbf{R}). \qquad (44)$$

F. On the convergence of the l_B expansion

Equation (44) above is clearly remarkable as it connects local vortex Green's function $g_{m;m'}(\mathbf{R})$ to the nonlocal electronic propagator $G(\mathbf{r},\mathbf{r}',\omega)$, from which all equilibrium physical properties can be obtained. Because the vortex wave functions appearing in this expression have a finite extension in space of order l_B, the combination of Eq. (44) with recursion relation (26), which encodes the small l_B expansion of $g_{m;m'}(\mathbf{R})$, allows one to systematically obtain *quantum* expressions for the physical observables, i.e., that are naively valid at small but finite magnetic length. In contrast, the usual semiclassical expansion[13,34,36] is formulated in a strict $l_B\to 0$ limit, which would appear in our formalism as a further expansion in powers of l_B of the wave functions in Eq.

(44). The latter semiclassical expansion, which is analyzed in detail in Secs. III D and IV D, is clearly asymptotic in nature and certainly fails to be accurate at low temperature, where quantum effects set in (this is explicitly demonstrated in Sec. V with the comparison to an exactly solvable model).

A central question is whether our expansion, performed order by order in powers of l_B for vortex Green's function $g(\mathbf{R})$, does fully capture the quantum effects that survive at small but nonzero magnetic length. As discussed by several authors,[10,12] the Schrödinger equation becomes integrable in this limit, with constants of motion associated to equipotential lines of the random potential. The wave functions are then localized on a scale l_B transverse to these equipotentials and spread on the whole constant energy contour. While this picture is certainly appealing, difficulties arise for generating a systematic expansion that takes into account Landau level mixing. In contrast, the vortex states are flexible enough to capture these important contributions but correspond to a starting point where wave functions are fully localized at the scale l_B. Indeed, the first term in our expansion [Eq. (29)] indicates that eigenstates in the $B=\infty$ limit correspond to equipotential points, not lines, and this is related to the fact that the vortex wave functions, which form an overcomplete basis, become pointlike and thus orthogonal in this limit. Physically, one expects that quantum fluctuations will play a crucial role as soon as B is finite by selecting orthogonal, and therefore more extended, wave packets. Mathematically, this phenomenon is reflected in our formalism by the presence of terms that have to be kept at each order of the small l_B expansion for vortex Green's functions [e.g., at order l_B^2, these are the terms with a single frequency ω_m in Eq. (35)]. The need for resumming this development comes, in fact, from the Taylor expansion to finite order of nonlocal vortex Green's function [Eqs. (22) and (43)]. Fortunately, as terms at an arbitrary order in l_B can be generated through relation (26), it is possible to achieve a resummation of the leading contributions to vortex Green's function. Although these considerations are beyond the scope of the present paper, a first step in this direction is presented for the case of the local electronic density in Sec. V D.

III. ELECTRON DENSITY

A. General expression

Vortex Green's functions being determined, one can then derive quantum microscopic expressions for the local physical observables. The equilibrium local density is related to distribution (lesser component) Green's function $G^<$ in the electronic representation by the general formula,

$$\rho(\mathbf{r}) = -i \int \frac{d\omega}{2\pi} G^<(\mathbf{r}, \mathbf{r}, \omega) \qquad (45)$$

$$= -i \int \frac{d\omega}{2\pi} \int \frac{d^2\mathbf{R}}{2\pi l_B^2} \sum_{m,m'} \Psi^*_{m',\mathbf{R}}(\mathbf{r}) \Psi_{m,\mathbf{R}}(\mathbf{r})$$

$$\times \sum_{k=0}^{+\infty} \frac{1}{k!} \left(-\frac{l_B^2}{2} \Delta_{\mathbf{R}} \right)^k g^<_{m;m'}(\mathbf{R}), \qquad (46)$$

where Eq. (44) has been used. The distribution function in the vortex basis reads at equilibrium,

$$-i g^<_{m;m'}(\mathbf{R}) = i n_F(\omega)[g^R_{m;m'}(\mathbf{R}) - g^A_{m;m'}(\mathbf{R})], \qquad (47)$$

$$n_F(\omega) = \frac{1}{1 + \exp[(\omega - \mu^*)/T]}, \qquad (48)$$

where the Fermi-Dirac distribution function has been introduced, with $\mu^*/e = \Phi_0$ as the electrochemical potential (which is constant in space at thermodynamic equilibrium).

The computation of the electronic density at an arbitrary order in the magnetic length expansion is now straightforward using Eq. (26) to generate successive contributions to $g^<_{m;m'}(\mathbf{R})$. An important remark is however in order. While Eq. (46) involves local Green's function relative to the vortex position $\mathbf{R}$, it takes into account all Landau level mixing processes (terms with $m \neq m'$). As we will discover in the following calculations, the combination of vortex wave functions $\Psi^*_{m',\mathbf{R}}(\mathbf{r})\Psi_{m,\mathbf{R}}(\mathbf{r})$ involves an extra power $l_B^{|m-m'|}$. For this reason, the contribution from $g^{(1)}$, which couples adjacent Landau levels, is actually of order l_B^2 and not l_B. Similarly, the diagonal ($m = m'$) terms in $g^{(2)}$ are indeed of order l_B^2, while contributions with $m = m' \pm 2$ [see Eq. (35)] are overall of order l_B^4 and will be discarded in the following.

B. Electron density at leading order

At leading order of the expansion in l_B, vortex Green's function is given by Eq. (29) so that the distribution function reads

$$-i g^{(0)<}_{m;m'}(\mathbf{R}) = 2\pi n_F(\omega) \delta_{m,m'} \delta[\omega - \xi_m(\mathbf{R})]. \qquad (49)$$

Inserting this in Eq. (46) and performing the frequency sum, we obtain the local electron density,

$$\rho^{(0)}(\mathbf{r}) = \int \frac{d^2\mathbf{R}}{2\pi l_B^2} \sum_{m=0}^{+\infty} |\Psi_{m,\mathbf{R}}(\mathbf{r})|^2 n_F[\xi_m(\mathbf{R})], \qquad (50)$$

$$|\Psi_{m,\mathbf{R}}(\mathbf{r})|^2 = \frac{1}{2\pi m! \, l_B^2} \left| \frac{\mathbf{R} - \mathbf{r}}{\sqrt{2} l_B} \right|^{2m} \exp\left[-\frac{(\mathbf{R} - \mathbf{r})^2}{2 l_B^2} \right]. \qquad (51)$$

We note that this zeroth order contribution (50) is already more powerful than the expression for the electron density that is obtained in the strict limit $l_B \to 0$ of infinite magnetic field,

$$\rho^{(0)}(\mathbf{r}) \to \frac{1}{2\pi l_B^2} \sum_{m=0}^{+\infty} n_F[\xi_m(\mathbf{r})]. \qquad (52)$$

This semiclassical result (52) has been widely used in the literature[19,36] as a basis to screening calculations. It however ignores the fact that the physical density cannot vary faster than the scale l_B as is clear from Eqs. (50) and (51), and this leads to important quantitative differences, especially at low temperatures where quantum smearing effects supersede the thermal broadening of the density.[30]

Thus, expression (50) clearly includes important resummations of a purely semiclassical development of the physi-

cal density such as Eq. (52), which is naturally encoded order by order in the expansion of vortex Green's functions. Before addressing the question of the convergence of both types of calculations in Secs. III D and IV D, we compute now the next order contribution to the density.

C. Electron density at order l_B^2

As mentioned above, the contribution of order l_B^2 to the density comes from three origins: the nondiagonal part of $g^{(1)}$, the diagonal part of $g^{(2)}$, and the term $\Delta_{\mathbf{R}} g^{(0)}$ in expression (46) appearing with $k=1$. Let us investigate these different contributions in turn.

1. Contribution from $g^{(1)}$

The contribution from $g^{(1)}$ is obtained by inserting Eq. (31) in Eq. (21) and reporting vortex Green's function in Eq. (46),

$$\rho^{(1)}(\mathbf{r}) = \int \frac{d^2\mathbf{R}}{2\pi l_B^2} \sum_{m=0}^{+\infty} \frac{l_B}{\sqrt{2}} \sqrt{m+1} \big[\Psi_{m+1,\mathbf{R}}^*(\mathbf{r})\Psi_{m,\mathbf{R}}(\mathbf{r})$$
$$\times (\partial_X V + i\partial_Y V) + \Psi_{m,\mathbf{R}}^*(\mathbf{r})\Psi_{m+1,\mathbf{R}}(\mathbf{r})(\partial_X V - i\partial_Y V) \big]$$
$$\times \frac{\{n_F[\xi_{m+1}(\mathbf{R})] - n_F[\xi_m(\mathbf{R})]\}}{\hbar\omega_c}. \tag{53}$$

It is useful to note the relation, proved in Appendix B,

$$\sqrt{m+1}\,\Psi_{m+1,\mathbf{R}}^*(\mathbf{r})\Psi_{m,\mathbf{R}}(\mathbf{r}) = -\frac{l_B}{\sqrt{2}}(\partial_x - i\partial_y)\sum_{p=0}^{m}|\Psi_{p,\mathbf{R}}(\mathbf{r})|^2, \tag{54}$$

which shows that the product of wave functions $\Psi_{m+1}^*\Psi_m$ with adjacent Landau indices generates terms that behave as l_B, so that the contribution from $g^{(1)}$ to the density is indeed of order l_B^2. Using Eq. (54), expression (53) can be written in the equivalent form,

$$\rho^{(1)}(\mathbf{r}) = -\int \frac{d^2\mathbf{R}}{2\pi l_B^2} \sum_{m=0}^{+\infty} \frac{\{n_F[\xi_{m+1}(\mathbf{R})] - n_F[\xi_m(\mathbf{R})]\}}{\hbar\omega_c}$$
$$\times l_B^2 \boldsymbol{\nabla}_{\mathbf{R}}V \cdot \sum_{p=0}^{m} \boldsymbol{\nabla}_{\mathbf{r}}|\Psi_{p,\mathbf{R}}(\mathbf{r})|^2. \tag{55}$$

Performing one of the discrete sums and an integration by parts and noting that $\boldsymbol{\nabla}_{\mathbf{r}}|\Psi_{m,\mathbf{R}}(\mathbf{r})|^2 = -\boldsymbol{\nabla}_{\mathbf{R}}|\Psi_{m,\mathbf{R}}(\mathbf{r})|^2$, we end up with

$$\rho^{(1)}(\mathbf{r}) = \int \frac{d^2\mathbf{R}}{2\pi l_B^2} \sum_{m=0}^{+\infty} |\Psi_{m,\mathbf{R}}(\mathbf{r})|^2 l_B^2 \left\{ n_F'[\xi_m(\mathbf{R})] \frac{|\boldsymbol{\nabla}_{\mathbf{R}}V|^2}{\hbar\omega_c} \right.$$
$$\left. + n_F[\xi_m(\mathbf{R})] \frac{\Delta_{\mathbf{R}}V}{\hbar\omega_c} \right\}. \tag{56}$$

2. Contribution from $g^{(2)}$

From Eq. (46) the remaining contributions to the electron density at order l_B^2 are clearly

$$\rho^{(2)}(\mathbf{r}) = -i\int \frac{d\omega}{2\pi} \int \frac{d^2\mathbf{R}}{2\pi l_B^2} \sum_m \Psi_{m,\mathbf{R}}^*(\mathbf{r})\Psi_{m,\mathbf{R}}(\mathbf{r}) \left[\frac{l_B^2}{2} g_{m;m}^{(2)<}(\mathbf{R}) \right.$$
$$\left. - \frac{l_B^2}{2} \Delta_{\mathbf{R}} g_{m;m}^{(0)<}(\mathbf{R}) \right]. \tag{57}$$

Using results (29) and (35), we obtain

$$\rho^{(2)}(\mathbf{r}) = \int \frac{d^2\mathbf{R}}{2\pi l_B^2} \sum_{m=0}^{+\infty} |\Psi_{m,\mathbf{R}}(\mathbf{r})|^2 \frac{l_B^2}{2} \left\{ n_F'[\xi_m(\mathbf{R})] \right.$$
$$\times \left(m\Delta_{\mathbf{R}}V - \frac{|\boldsymbol{\nabla}_{\mathbf{R}}V|^2}{\hbar\omega_c} \right) - n_F''[\xi_m(\mathbf{R})] \frac{|\boldsymbol{\nabla}_{\mathbf{R}}V|^2}{2}$$
$$+ \frac{|\boldsymbol{\nabla}_{\mathbf{R}}V|^2}{(\hbar\omega_c)^2} \{(m+1)n_F[\xi_{m+1}(\mathbf{R})] - (2m+1)n_F[\xi_m(\mathbf{R})]$$
$$\left. + mn_F[\xi_{m-1}(\mathbf{R})]\} \right\}. \tag{58}$$

The components $\delta_{m,m'\pm 2}$ of the function $g^{(2)}$ [see Eq. (35)] have not been included in the calculations since they generate corrections to the density of the order l_B^4.

The final results for the electronic density up to order l_B^2, given in formulas (50), (56), and (58), will be exploited in detail by a comparison with an exactly solvable model in Sec. V. In anticipation to Sec. V D, we note that all these expressions require at very low temperature a resummation procedure, which leads to define renormalized energies and wave functions.

D. Semiclassical density: The strict $l_B \to 0$ expansion

As already mentioned above, it is possible to express the electron density under the form of a strict expansion in powers of the magnetic length. This corresponds exactly to a systematic semiclassical development with respect to the center-of-mass motion (the orbital motion giving rise to the Landau levels is always treated quantum mechanically).

In this section, we write down explicitly the first corrections to the well-known semiclassical expression, i.e., Eq. (52), for the electron density. Nonlocal expressions (50), (56), and (58) can be transformed into local ones, in a similar way as has been done at the level of the Dyson equation [Eq. (11)], by replacing any integral over the vortex position $\mathbf{R}$ in the following way:

$$\int d^2\mathbf{R}|\Psi_{m,\mathbf{R}}(\mathbf{r})|^2 f(\mathbf{R}) = \int d^2\mathbf{R}|\Psi_{m,\mathbf{R}}(\mathbf{0})|^2 f(\mathbf{r}+\mathbf{R})$$
$$= \int d^2\mathbf{R}|\Psi_{m,\mathbf{R}}(\mathbf{0})|^2 \sum_{j=0}^{+\infty} \frac{(\mathbf{R}\cdot\boldsymbol{\nabla}_{\mathbf{r}})^j}{j!} f(\mathbf{r}), \tag{59}$$

$$= \sum_{j=0}^{+\infty} \frac{(m+j)!}{(j!)^2 m!} \left(\frac{l_B^2}{2}\Delta_{\mathbf{r}} \right)^j f(\mathbf{r}), \tag{60}$$

where $f(\mathbf{R})$ represents an arbitrary function of the vortex position. Using Eq. (60) in Eq. (50), we get the semiclassical

contribution of order l_B^2 arising from the expansion of $\rho^{(0)}$,

$$\rho^{(0)}(\mathbf{r}) = \frac{1}{2\pi l_B^2}\sum_{m=0}^{+\infty}\left\{n_F[\xi_m(\mathbf{r})] + \frac{l_B^2}{2}(m+1)\Delta_\mathbf{r}n_F[\xi_m(\mathbf{r})]\right\}. \tag{61}$$

At order l_B^2, the contribution from $\rho^{(1)}$ [Eq. (56)] is readily obtained as

$$\rho^{(1)}(\mathbf{r}) = \frac{1}{2\pi l_B^2}\sum_{m=0}^{+\infty}l_B^2\left\{n_F'[\xi_m(\mathbf{r})]\frac{|\boldsymbol{\nabla}_\mathbf{r}V|^2}{\hbar\omega_c} + n_F[\xi_m(\mathbf{r})]\Delta_\mathbf{r}V\right\}. \tag{62}$$

Similarly, the contribution from $\rho^{(2)}$ [Eq. (58)] reads after simplification,

$$\rho^{(2)}(\mathbf{r}) = \frac{1}{2\pi l_B^2}\sum_{m=0}^{+\infty}\frac{l_B^2}{2}\left\{n_F'[\xi_m(\mathbf{r})]\left(m\Delta_\mathbf{r}V - \frac{|\boldsymbol{\nabla}_\mathbf{r}V|^2}{\hbar\omega_c}\right)\right.$$
$$\left. - n_F''[\xi_m(\mathbf{r})]\frac{|\boldsymbol{\nabla}_\mathbf{r}V|^2}{2}\right\}. \tag{63}$$

Collecting all the different contributions, we find that the total electronic density in high magnetic fields including the first quantum corrections of order l_B^2 is given by

$$\rho(\mathbf{r}) = \frac{1}{2\pi l_B^2}\sum_{m=0}^{+\infty}n_F[\xi_m(\mathbf{r})] + \frac{1}{2\pi l_B^2}\sum_{m=0}^{+\infty}l_B^2\left\{n_F[\xi_m(\mathbf{r})]\frac{\Delta_\mathbf{r}V}{\hbar\omega_c}\right.$$
$$+ \left(m+\frac{1}{2}\right)n_F'[\xi_m(\mathbf{r})]\Delta_\mathbf{r}V + \frac{1}{2}n_F'[\xi_m(\mathbf{r})]\frac{|\boldsymbol{\nabla}_\mathbf{r}V|^2}{\hbar\omega_c}$$
$$\left. + \frac{1}{2}\left(m+\frac{1}{2}\right)n_F''[\xi_m(\mathbf{r})]|\boldsymbol{\nabla}_\mathbf{r}V|^2\right\}. \tag{64}$$

In order to physically interpret this result, we can alternatively write

$$\rho(\mathbf{r}) = \frac{1}{2\pi l_B^2}\sum_{m=0}^{+\infty}\left\{n_F[\widetilde{\xi}_m(\mathbf{r})] + l_B^2 n_F[\xi_m(\mathbf{r})]\frac{\Delta_\mathbf{r}V}{\hbar\omega_c}\right.$$
$$\left. + l_B^2 n_F'[\xi_m(\mathbf{r})]\frac{|\boldsymbol{\nabla}_\mathbf{r}V|^2}{\hbar\omega_c} + \frac{l_B^2}{2}\left(m+\frac{1}{2}\right)\Delta_\mathbf{r}n_F[\xi_m(\mathbf{r})]\right\}, \tag{65}$$

where corrections proportional to n_F' in $\rho^{(2)}$ have been absorbed into renormalized Landau-level energies as

$$\widetilde{\xi}_m(\mathbf{r}) = \xi_m(\mathbf{r}) + \frac{l_B^2}{2}\left(m+\frac{1}{2}\right)\Delta_\mathbf{r}V - \frac{l_B^2}{2}\frac{|\boldsymbol{\nabla}_\mathbf{r}V|^2}{\hbar\omega_c}. \tag{66}$$

These semiclassical energies [Eq. (66)] have been previously found in the literature[13,34] with techniques based on effective Hamiltonians, which neglect Landau level mixing, and thus do not allow one to compute full local-density expression (65). The second term appearing in the rhs of Eq. (65), proportional to $l_B^2 n_F\Delta_\mathbf{r}V/\hbar\omega_c$, reflects the small but nonzero compressibility of the electron gas even in the absence of electron-electron interaction. This term and also the third term in Eq. (65), both derived from $g^{(1)}$, stem from adjacent

Landau level mixing processes and can be interpreted as small corrections to the wave function for a smooth potential $V(\mathbf{r})$. Clearly, the fourth term in Eq. (65), proportional to $l_B^2\Delta_\mathbf{r}n_F$, is only a small correction if the electronic density is also smooth at the scale of l_B. This indicates that the semiclassical picture breaks down at low temperature. In this case, one has to resort to fully quantum expressions such as Eqs. (50), (56), and (58), as will be discussed in Sec. V C.

E. Electron-electron interactions and screening

As a result of electron-electron interactions, the potential V entering into the previous expressions through the Fermi function is possibly very different from the bare electrostatic potential (related to confining gates and random impurities outside the bidimensional electron gas) and has to be determined self-consistently from screening theory. Previous work, rooted in the semiclassical picture, used expressions for the electron density such as Eq. (52) as a starting point for Thomas-Fermi type of calculations.[19,20,37] The physical picture that emerged from these studies is that the sample separates into either compressible regions, where screening of the bare potential is almost perfect and the electronic density varies spatially, or into incompressible regions, where the density is almost exactly pinned and the gradient of the effective potential is nonzero. Further work[30] has however shown that important deviations result from a better resolution of the self-consistent problem within a Hartree approximation that includes quantum smearing effects from the electronic wave functions. Most of these calculations are performed in simplified one-dimensional geometries, since the self-consistent resolution of the Schrödinger equation becomes prohibitive for an arbitrary disorder landscape.[27,38] One can hope that our high-field expression for the density will turn out to be a very useful tool in this context of the study of electron-electron interaction effects in a disordered system.

IV. ELECTRON CURRENT DENSITY

A. General expression

The local electron current density is defined in terms of electronic Green's function by

$$\mathbf{j}(\mathbf{r},\omega) = \left[\frac{e\hbar}{2m^*}(\boldsymbol{\nabla}_{\mathbf{r}'} - \boldsymbol{\nabla}_\mathbf{r}) + i\frac{e^2}{m^*c}\mathbf{A}\right]G^<(\mathbf{r},\mathbf{r}',\omega)\bigg|_{\mathbf{r}'=\mathbf{r}}. \tag{67}$$

In a first step, this expression can be written in terms of vortex Green's functions. Inserting expression (44), we get

$$\mathbf{j}(\mathbf{r},\omega) = \frac{e\hbar}{2m^*}\int\frac{d^2\mathbf{R}}{2\pi l_B^2}\sum_{m,m'}\left[\Psi_{m,\mathbf{R}}(\mathbf{r})\boldsymbol{\nabla}_\mathbf{r}\Psi_{m',\mathbf{R}}^*(\mathbf{r})\right.$$
$$- \Psi_{m',\mathbf{R}}^*(\mathbf{r})\boldsymbol{\nabla}_\mathbf{r}\Psi_{m,\mathbf{R}}(\mathbf{r}) + 2i\frac{e}{\hbar c}\mathbf{A}\Psi_{m',\mathbf{R}}^*(\mathbf{r})\Psi_{m,\mathbf{R}}(\mathbf{r})\bigg]$$
$$\times\sum_{k=0}^{+\infty}\frac{1}{k!}\left(-\frac{l_B^2}{2}\Delta_\mathbf{R}\right)^k g_{m,;m'}^<(\mathbf{R},\omega). \tag{68}$$

The dependence on the variable $\mathbf{r}$ is contained only in the wave functions and the vector potential $\mathbf{A}$, which are all known (we remind that we have chosen the symmetrical gauge to write down explicitly the vortex wave functions). Using the relation

$$\boldsymbol{\nabla}_{\mathbf{r}}\Psi_m = \begin{pmatrix} \dfrac{\sqrt{m}}{\sqrt{2}l_B}\Psi_{m-1} - \dfrac{\sqrt{m+1}}{\sqrt{2}l_B}\Psi_{m+1} + \dfrac{iy}{2l_B^2}\Psi_m \\[2ex] i\dfrac{\sqrt{m}}{\sqrt{2}l_B}\Psi_{m-1} + i\dfrac{\sqrt{m+1}}{\sqrt{2}l_B}\Psi_{m+1} - \dfrac{ix}{2l_B^2}\Psi_m \end{pmatrix}, \tag{69}$$

we can rewrite the bracketed term in Eq. (68) as

$$i\boldsymbol{\nabla}_{\mathbf{r}}[\Psi_{m,\mathbf{R}}(\mathbf{r})\Psi^*_{m',\mathbf{R}}(\mathbf{r})] \times \hat{\mathbf{z}} - \frac{\sqrt{2}}{l_B}\begin{pmatrix} \sqrt{m'+1}\Psi_{m,\mathbf{R}}(\mathbf{r})\Psi^*_{m'+1,\mathbf{R}}(\mathbf{r}) - \sqrt{m+1}\Psi_{m+1,\mathbf{R}}(\mathbf{r})\Psi^*_{m',\mathbf{R}}(\mathbf{r}) \\[1ex] i\sqrt{m'+1}\Psi_{m,\mathbf{R}}(\mathbf{r})\Psi^*_{m'+1,\mathbf{R}}(\mathbf{r}) + i\sqrt{m+1}\Psi_{m+1,\mathbf{R}}(\mathbf{r})\Psi^*_{m',\mathbf{R}}(\mathbf{r}) \end{pmatrix}. \tag{70}$$

Inserting expression (70) in formula (68), we finally get our starting point for the computation of the current density,

$$\mathbf{j}(\mathbf{r},\omega) = \frac{e\hbar}{2m^*}\Bigg[\hat{\mathbf{z}} \times \boldsymbol{\nabla}_{\mathbf{r}}\rho(\mathbf{r},\omega) - \frac{\sqrt{2}}{l_B}\int \frac{d^2\mathbf{R}}{2\pi l_B^2}\sum_{m,m'}\begin{pmatrix} \sqrt{m'+1}\Psi_{m,\mathbf{R}}(\mathbf{r})\Psi^*_{m'+1,\mathbf{R}}(\mathbf{r}) - \sqrt{m+1}\Psi_{m+1,\mathbf{R}}(\mathbf{r})\Psi^*_{m',\mathbf{R}}(\mathbf{r}) \\[1ex] i\sqrt{m'+1}\Psi_{m,\mathbf{R}}(\mathbf{r})\Psi^*_{m'+1,\mathbf{R}}(\mathbf{r}) + i\sqrt{m+1}\Psi_{m+1,\mathbf{R}}(\mathbf{r})\Psi^*_{m',\mathbf{R}}(\mathbf{r}) \end{pmatrix}$$

$$\times \sum_{k=0}^{+\infty}\frac{1}{k!}\left(-\frac{l_B^2}{2}\Delta_{\mathbf{R}}\right)^k g^<_{m;m'}(\mathbf{R},\omega)\Bigg], \tag{71}$$

where $\rho(\mathbf{r},\omega)=-iG^<(\mathbf{r},\mathbf{r},\omega)$ is the local spectral function. Similar to Sec. III, we wish to collect all contributions up to order l_B^2 to the local current density.

B. Electronic current at leading order

The procedure to compute the different contributions to the current density is completely analogous to the calculation of the electronic density done in Sec. III, although more lengthy. The leading contributions are easily seen in Eq. (71) to come from $g^{(0)}$ and $g^{(1)}$.

1. Contribution from $g^{(0)}$: Density-gradient current

Leading-order Green's function is purely diagonal with respect to the Landau-level index m, so that we have to consider combinations as $\sqrt{m+1}\Psi_m\Psi^*_{m+1}$ in Eq. (71). Inserting both $\rho^{(0)}$ from Eq. (50) and $g^{(0)}$ from Eq. (29) (considering only the contribution with $k=0$) and using useful relation (54), we readily obtain after the frequency integral

$$\mathbf{j}^{(0)}(\mathbf{r}) = -\frac{e}{h}\hat{\mathbf{z}} \times \boldsymbol{\nabla}_{\mathbf{r}}\int \frac{d^2\mathbf{R}}{2\pi l_B^2}\sum_{m=0}^{+\infty}\hbar\omega_c n_F[\xi_m(\mathbf{R})]$$

$$\times \left[\sum_{p=0}^{m}|\Psi_{p,\mathbf{R}}(\mathbf{r})|^2 - \frac{|\Psi_{m,\mathbf{R}}(\mathbf{r})|^2}{2}\right]. \tag{72}$$

This contribution to the current density has the property that its volume average vanishes: $\int d^2\mathbf{r}\,\mathbf{j}^{(0)}(\mathbf{r})=0$.

As done previously for the local electronic density, density-gradient contribution (72) can be expanded in the strict $l_B\to 0$ limit to recover a semiclassical expression,

$$\mathbf{j}^{(0)}(\mathbf{r}) = \frac{e}{h}\sum_{m=0}^{+\infty}\left(m+\frac{1}{2}\right)\hbar\omega_c\boldsymbol{\nabla}_{\mathbf{r}}n_F[\xi_m(\mathbf{r})] \times \hat{\mathbf{z}}. \tag{73}$$

This result coincides with the formula for the "edge" electronic current density derived within a different method in Ref. 36. It has clearly the form of a current flow responding to a gradient of the density. It thus vanishes in the incompressible regions where the density is quasiconstant and becomes important in the compressible regions of the system where the local density is strongly inhomogeneous and the bare potential is almost perfectly screened. Such regions are not necessarily located at the edges of the system but are rather spread throughout the system. The denomination of "edge current" is thus in some sense abusive. Therefore, we prefer to call contributions (72) and (73) a density-gradient current.

2. Contribution from $g^{(1)}$: Drift current

As emphasized in our previous paper,[35] the well-known drift contribution to the current density appears, in fact, beyond the limit $l_B\to 0$, i.e., when considering Green's functions $g^{(1)}$ which take into account the first processes of Landau level mixing. Such a drift contribution is however of the same order as the density-gradient contribution [the reason is that there is a prefactor l_B^{-1} in the general expression of the current density, see the second term in the right-hand side of Eq. (71)].

Using the general expression for current density (71) with $k=0$ and inserting $g^{(1)}$ from Eq. (31), we get

$$\mathbf{j}^{(1)}(\mathbf{r}) = \frac{e\hbar}{2m^*}\hat{\mathbf{z}} \times \boldsymbol{\nabla}_{\mathbf{r}}\rho^{(1)}(\mathbf{r})$$

$$+ \frac{e\hbar}{m^*}\int \frac{d^2\mathbf{R}}{2\pi l_B^2}\sum_{m=0}^{+\infty} \frac{n_F[\xi_{m+1}(\mathbf{R})] - n_F[\xi_m(\mathbf{R})]}{\hbar\omega_c}\Bigg[(m+1)$$

$$\times |\Psi_{m+1,\mathbf{R}}(\mathbf{r})|^2 \hat{\mathbf{z}} \times \boldsymbol{\nabla}_{\mathbf{R}}V(\mathbf{R}) + \sqrt{m+1}\sqrt{m+2}$$

$$\times \binom{\mathrm{Im}}{\mathrm{Re}}(\partial_X V + i\partial_Y V)\Psi_{m,\mathbf{R}}(\mathbf{r})\Psi^*_{m+2,\mathbf{R}}(\mathbf{r})\Bigg]. \qquad (74)$$

In Appendix C we provide a detailed calculation of this expression (74), which contains a peculiar term (the last one) involving vortex wave functions with Landau indices that differ by 2. As a result, we find that the leading contribution to Eq. (74) reads

$$\mathbf{j}^{(1)}(\mathbf{r}) = \frac{e}{h}\int d^2\mathbf{R}\sum_{m=0}^{+\infty} |\Psi_{m,\mathbf{R}}(\mathbf{r})|^2 n_F[\xi_m(\mathbf{R})]\boldsymbol{\nabla}_{\mathbf{R}}V(\mathbf{R}) \times \hat{\mathbf{z}}. \qquad (75)$$

In the limit $l_B \rightarrow 0$, above contribution (75) yields

$$\mathbf{j}^{(1)}(\mathbf{r}) = \frac{e}{h}\sum_{m=0}^{+\infty} n_F[\xi_m(\mathbf{r})]\boldsymbol{\nabla}_{\mathbf{r}}V(\mathbf{r}) \times \hat{\mathbf{z}}. \qquad (76)$$

We thus recover the well-known drift current that can be found in the literature,[36] while expression (75) constitutes a quantum version of this drift current, which may be used at low temperature.

C. Electronic current at order l_B^2

We aim at collecting exhaustively all contributions to the current density that are proportional to l_B^2: this is the order where the first dissipative features are expected to appear (see Sec. VI). We will simply list here the various origins for these terms and refer the reader to Appendix C for the detailed calculation.

There is first a subdominant contribution coming from $g^{(1)}$, with expression (74). In Appendix C this contribution is denoted $\mathbf{j}^{(1)}_{\mathrm{sub}}$ and is given in Eq. (C6). Another contribution of order l_B^2 arises with second-order Green's function $g^{(2)}$. The latter contains diagonal elements ($m = m'$) that combine with the first and second terms in the right-hand side of Eq. (71) and also off-diagonal elements $\delta_{m,m'\pm2}$, which have to be inserted in the second term of the right-hand side of Eq. (71). The final expression for $\mathbf{j}^{(2)}$, which also includes the contribution from the function $g^{(0)}$ appearing with the term $k=1$ in Eq. (71), is given by Eq. (C8). Finally, the off-diagonal elements $\delta_{m,m'\pm1}$ of $g^{(3)}$, calculated in Appendix A, combine with the contribution from the function $g^{(1)}$ associated with the term $k=1$ in Eq. (71), giving the final result for $\mathbf{j}^{(3)}$ in Eq. (C10).

D. Semiclassical current: The strict $l_B \rightarrow 0$ expansion

As previously done with the local electronic density, it is also possible to express the current density under the form of a strict expansion in powers of the magnetic length. In this section, we want to obtain the corrections of order l_B^2 to the well-known semiclassical expression (76) for the drift current, which is purely transverse. All these subleading contributions are collected in Appendix C. Since the semiclassical expansion in l_B is only valid in a "high" temperature regime, we will only present here the terms proportional to the Fermi factor that are dominant in this regime with respect to the other terms involving derivatives of the Fermi factor.

Collecting Eq. (76) with the contributions from Eqs. (C11)–(C14), we get the leading contribution to the semiclassical current,

$$\mathbf{j}(\mathbf{r}) = \frac{e}{h}\sum_{m=0}^{+\infty} n_F[\xi_m(\mathbf{r})]\Bigg[\boldsymbol{\nabla}_{\mathbf{r}}V + l_B^2\frac{(\boldsymbol{\nabla}_{\mathbf{r}}V \cdot \boldsymbol{\nabla}_{\mathbf{r}})}{\hbar\omega_c}\boldsymbol{\nabla}_{\mathbf{r}}V$$

$$+ \frac{3}{2}l_B^2\left(m+\frac{1}{2}\right)\Delta\boldsymbol{\nabla}_{\mathbf{r}}V\Bigg] \times \hat{\mathbf{z}}. \qquad (77)$$

This expression constitutes one of the main physical results of the paper and is further analyzed in Sec. IV dealing with the nonequilibrium transport properties.

V. CHECKING OUR THEORY: COMPARISONS WITH AN EXACTLY SOLVABLE CASE

A. One-dimensional parabolic confinement model

The aim of this section is to benchmark our results for the local equilibrium charge and current densities obtained with the vortex states. For this purpose a comparison to the exact solution that can be obtained for the case of a one-dimensional parabolic confining potential turns out to be quite enlightening. We will therefore focus here on the following potential profile:

$$V(x) = \frac{1}{2}m^*\omega_0^2 x^2. \qquad (78)$$

Following Ref. 36, the exact eigenstates and eigenenergies corresponding to this particular choice of one-dimensional potential are given in the Landau gauge $\mathbf{A} = Bx\hat{\mathbf{y}}$ by

$$\Psi_{np}(\mathbf{r}) = \frac{e^{-ipy}e^{-[x-(\omega_c/\Omega)pL^2]^2/2L^2}}{\sqrt{2^{n+1}n!\,\pi^{3/2}L}}H_n\left(\frac{x-\frac{\omega_c}{\Omega}pL^2}{L}\right), \qquad (79)$$

$$E_{np} = \hbar\Omega\left(n+\frac{1}{2}\right) + V(pL^2), \qquad (80)$$

where $\Omega = \sqrt{\omega_c^2 + \omega_0^2}$ and $L = \sqrt{\hbar/m^*\Omega}$ are the renormalized cyclotron pulsation and magnetic length, respectively, and H_n denotes the nth Hermite polynomial. These wave functions, fully extended plane waves along constant energy contour while strongly localized in the transverse x direction, are certainly very different from the vortex states [Eq. (2)],

which are localized in all directions without preferred symmetry, so that this comparison provides a very stringent test on the vortex theory.

Physical observables, such as the local electronic density, are readily obtained as

$$\rho(x) = \sum_{n=0}^{+\infty} \int_{-\infty}^{+\infty} dp |\Psi_{np}(\mathbf{r})|^2 n_F(E_{np}), \tag{81}$$

while the equilibrium current density, directed in the y direction, reads[36]

$$j(x) = \sum_{n=0}^{+\infty} \int_{-\infty}^{+\infty} dp j_{np}(x) n_F(E_{np}), \tag{82}$$

where

$$j_{np}(x) = \frac{|e|\Omega^2}{\omega_c} \left(\frac{\omega_c}{\Omega} pL^2 - x \right) |\Psi_{np}(\mathbf{r})|^2 + |e|\omega_c l_B^2 \frac{V'(x)}{\hbar\omega_c} |\Psi_{np}(\mathbf{r})|^2. \tag{83}$$

B. Checking analytically the semiclassical expansion

The first check, which is crucial for demonstrating the mathematical consistency of our semiclassical limit, as obtained from the vortex calculation, consists in developing both Eqs. (81) and (83) in a strict magnetic length expansion at order l_B^2. For this purpose, we develop Ω and L using $\omega_0^2/\omega_c^2 = l_B^2 V''(x)/\hbar\omega_c$ and perform a Taylor expansion. The resulting Gaussian integrals are computed using the formula

$$\int_{-\infty}^{+\infty} d\xi e^{-\xi^2} \xi^2 H_n^2(\xi) = \sqrt{\pi} 2^n n! \left(n + \frac{1}{2} \right). \tag{84}$$

This leads to the result

$$\rho(x) = \frac{1}{2\pi l_B^2} \sum_{n=0}^{+\infty} \left[n_F(x) + l_B^2 n_F(x) \frac{V''(x)}{\hbar\omega_c} + l_B^2 n_F'(x) V''(x) \right. $$
$$\left. + \frac{l_B^2}{2} n_F'(x) \frac{[V'(x)]^2}{\hbar\omega_c} + \frac{l_B^2}{2} \left(n + \frac{1}{2} \right) n_F''(x) [V'(x)]^2 \right], \tag{85}$$

where $n_F(x) = n_F[(n+1/2)\hbar\omega_c + V(x)]$, which is obviously equivalent to Eq. (64).

The calculation of the semiclassical current density at order l_B^2 follows the same lines, and using formula

$$\int_{-\infty}^{+\infty} d\xi e^{-\xi^2} \xi^4 H_n^2(\xi) = 3\sqrt{\pi} 2^{n-1} n! (n^2 + n + 1/2), \tag{86}$$

we recover the leading density-gradient and drift contributions,

$$j_0(x) = \frac{|e|}{h} \sum_{n=0}^{+\infty} \left[n_F(x) V' + \left(n + \frac{1}{2} \right) \hbar\omega_c n_F'(x) V' \right], \tag{87}$$

while the terms of order l_B^2 read

$$j_2(x) = \frac{|e|}{h} l_B^2 \sum_{n=0}^{+\infty} \left[\frac{n_F'''(x)}{4} (n^2 + n + 1/2) \hbar\omega_c (V')^3 + n_F''(x) \right.$$
$$\times \left(\frac{5}{4} n^2 + \frac{5}{4} n + \frac{1}{2} \right) V' V'' \hbar\omega_c + n_F'(x) \frac{(V')^3}{2\hbar\omega_c}$$
$$+ n_F''(x) \left(n + \frac{1}{2} \right) (V')^3 + n_F'(x) \frac{7}{2} \left(n + \frac{1}{2} \right) V' V''$$
$$\left. + n_F(x) V' \frac{V''}{\hbar\omega_c} \right]. \tag{88}$$

One can easily check that collecting all terms in expressions (C11)–(C14) for a one-dimensional potential yields the same result, giving a good confidence in the vortex method to generate the semiclassical expansion. We emphasize however that our semiclassical results were derived for an arbitrary two-dimensional potential, so that extra terms are actually present in our semiclassical formula with respect to Eq. (88). In particular some of the terms appearing in Eq. (77) involve derivatives of the potential in two orthogonal directions and cannot be inferred from this simple calculation of a one-dimensional parabolic potential. It is interesting to note that in nonequilibrium it is precisely these additional terms in the current density that are seemingly associated with dissipative features (see Sec. VI).

C. Systematic numerical comparison to the vortex theory

We aim here at giving a more quantitative comparison for the electronic density between the exactly solvable model and the various developments discussed in Sec. III. We therefore compute numerically expression (81) and investigate both the semiclassical approximation (52) and the order l_B^2 quantum expressions (50) and (58). Note that the l_B^2 corrections [Eq. (64)] to the semiclassical result present derivatives of the Fermi factor, which are either very small (at high temperatures) or very singular at low temperatures, so that they are not included in the comparison. In contrast, the l_B^2 corrections [Eq. (58)] to leading quantum result (50) are more regular, and their inclusion is important to reach quantitative agreement in an intermediate temperature range, as we will demonstrate below.

In order to show that the reliability of these different approximation schemes is rooted in specific temperature regimes, we present results for different temperatures at a given confinement energy $\hbar\omega_0 = \omega_c/5$, small enough to ensure the smoothness of the external potential yet already sufficiently large so that the semiclassical approximation is in trouble at low temperature. The electrochemical potential is also fixed by taking $\mu^* = 3\omega_c$, so that three Landau levels are present at the center of the system.

At temperatures not too low compared to the cyclotron frequency [first panel (a) of Fig. 1 for $k_B T = 0.2\hbar\omega_c$], the semiclassical result is still close to the exact solution, exactly matched by the quantum result. Lowering further the temperature [second panel (b) of Fig. 1 for $k_B T = 0.1\hbar\omega_c$] shows increasing deviations with the semiclassical result, while the complicated variations in the exact density are perfectly re-
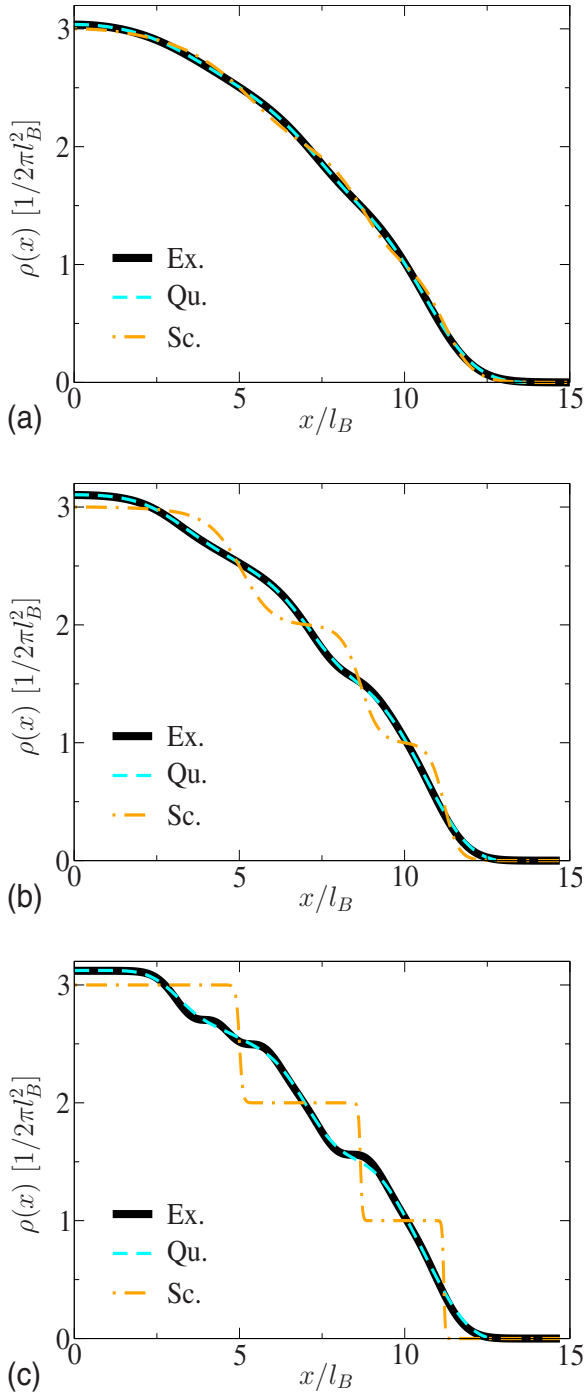
FIG. 1. (Color online) Local electronic density $\rho(x)$ in units of $1/2\pi l_B^2$ for the one-dimensional parabolic potential with $\omega_0 = \omega_c/5$ and $\mu^* = 3\omega_c$, as a function of x/l_B, comparing exact expression (81) (solid curve, label Ex.) with semiclassical expansion (52) (dotted-dashed curved, label Sc.) and the quantum expansion given by Eqs. (50), (56), and (58) (dashed curve, label Qu.). The three different panels (a)–(c) correspond to decreasing temperatures $k_B T/\hbar\omega_c$ = 0.2, 0.1, and 0.01.

produced by the quantum formula. In particular, both the small compressibility in the filling factor $n=3$ plateau [the density of the third filled Landau level is slightly greater than the value $3 \times (2\pi l_B^2)^{-1}$] and the broad smearing of the $n=1$

and $n=2$ plateaus are quantitatively described. In the very low-temperature regime, small shoulders appear at fractional densities [panel (c) of Fig. 1 for $k_B T = 0.01\hbar\omega_c$], which are associated with the zeros of the Hermite polynomials in Eq. (79). These variations are only partially reproduced by the quantum expression, but the overall agreement remains very good.

D. Zero temperature limit: Resummation of the quantum development

We finally motivate the need for a resummation of the quantum expression to arbitrary order in l_B in the very low-temperature regime, as hinted in Sec. II F. As the semiclassical expression for electronic density (65) is clearly divergent at low temperature, one can indeed ask whether the leading quantum result (50) and its order l_B^2 corrections (56) and (58) give satisfactory results for all temperatures. Despite the excellent agreement observed above, the Fermi factor derivatives appearing in these order l_B^2 terms tend to give important and uncontrolled contributions in the zero-temperature limit. To see this, let us forget for the time being the (negligible) terms inversely proportional to $\hbar\omega_c$ in the quantum expression for the density, which then simply reads

$$\rho(\mathbf{r}) = \int \frac{d^2\mathbf{R}}{2\pi l_B^2} \sum_{m=0}^{+\infty} |\Psi_{m,\mathbf{R}}(\mathbf{r})|^2 \left\{ n_F[\xi_m(\mathbf{R})] - \frac{l_B^2}{4}\Delta_\mathbf{R} n_F[\xi_m(\mathbf{R})] \right\},$$
(89)

$$= \rho^{(0)}(\mathbf{r}) - \frac{l_B^2}{4}\Delta_\mathbf{r}\rho^{(0)}(\mathbf{r}).$$
(90)

Here we have made an integration by parts to rewrite the second term in the rhs of Eq. (89). Because $\rho^{(0)}$ cannot change on a scale smaller than l_B, as is clear from Eq. (50), the l_B^2 correcting term in the rhs of Eq. (90) cannot become singular in the zero-temperature limit, in contrast to semiclassical expression (65). However, $\rho^{(0)}$ does change on the scale l_B at the boundary of an incompressible region at very low temperature, so that the correction becomes of order one and needs to be resummed to all orders. The need for a resummation is mathematically related to the fact that non-local vortex Green's function has been developed at coinciding points in Eq. (22) while keeping a finite number of contributions. A clear example of such a nonlocal resummation to all orders is relation (44) between vortex and electron propagators. In fact, the correction in Eq. (90) is the combination of the $-(l_B^2/2)\Delta_\mathbf{R} g^{(0)}$ term in Eq. (44) and the $(l_B^2/4)\Delta_\mathbf{R} g^{(0)}$ contribution that can be extracted from $g^{(2)}$ in Eq. (35).

By inspecting recursion relation (26) in the small l_B limit, it is possible to infer that this class of most singular terms in the vortex propagator is given *to all orders* by

$$g_{m;m'}^{B\to\infty}(\mathbf{R}) = \delta_{m,m'} \sum_{k=0}^{+\infty} \frac{1}{k!} \left(\frac{l_B^2}{4}\Delta_\mathbf{R}\right)^k g_{m;m}^{(0)}(\mathbf{R}),$$
(91)

so that their combination with Eq. (44) leads to the final quantum expression for the density in the small but nonzero l_B limit,

$$\rho^{B \to \infty}(\mathbf{r}) = \int \frac{d^2\mathbf{R}}{2\pi l_B^2} \sum_{m=0}^{+\infty} |\Psi_{m,\mathbf{R}}(\mathbf{r})|^2$$

$$\times \sum_{k=0}^{+\infty} \frac{1}{k!} \left(-\frac{l_B^2}{4} \Delta_{\mathbf{R}} \right)^k n_F[\xi_m(\mathbf{R})]. \qquad (92)$$

Using an integration by parts, this equation can be written in the equivalent form,

$$\rho^{B \to \infty}(\mathbf{r}) = \int \frac{d^2\mathbf{R}}{2\pi l_B^2} \sum_{m=0}^{+\infty} n_F[\xi_m(\mathbf{R})]$$

$$\times \sum_{k=0}^{+\infty} \frac{1}{k!} \left(-\frac{l_B^2}{4} \Delta_{\mathbf{R}} \right)^k |\Psi_{m,\mathbf{R}}(\mathbf{r})|^2. \qquad (93)$$

We note from Fourier analysis that the differential operator

$$\sum_{k=0}^{+\infty} \frac{1}{k!} \left(-\frac{l_B^2}{4} \Delta_{\mathbf{R}} \right)^k$$

is nothing else than a convolution operator with the kernel $e^{-\mathbf{u}^2/4t}/(4\pi t)$, where $t = -l_B^2/4$. We can apply this to the vortex density to find

$$\rho^{B \to \infty}(\mathbf{r}) = \int \frac{d^2\mathbf{R}}{2\pi l_B^2} \sum_{m=0}^{+\infty} n_F[\xi_m(\mathbf{R})] |\Phi_{m,\mathbf{R}}(\mathbf{r})|^2, \qquad (94)$$

$$|\Phi_{m,\mathbf{R}}(\mathbf{r})|^2 = \int \frac{d^2\mathbf{u}}{4\pi t} e^{-\mathbf{u}^2/4t} |\Psi_{m,\mathbf{R}-u}(\mathbf{r})|^2. \qquad (95)$$

Performing formally the remaining Gaussian integral over $\mathbf{u}$ in Eq. (95), we find

$$\rho^{B \to \infty}(\mathbf{r}) = \int \frac{d^2\mathbf{R}}{2\pi l_B^2} \sum_{m=0}^{+\infty} \frac{n_F[\xi_m(\mathbf{R})]}{\pi m! \, l_B^2} A_m(\mathbf{R} - \mathbf{r})$$

$$\times \exp\left[-\frac{(\mathbf{R} - \mathbf{r})^2}{l_B^2} \right], \qquad (96)$$

where A_m is the following polynomial:

$$A_m(\mathbf{R}) = \frac{\partial^m}{\partial s^m} \left(\frac{1}{1+s} \exp\left[\frac{\mathbf{R}^2}{l_B^2} \frac{2s}{1+s} \right] \right)_{s=0}. \qquad (97)$$

Final expression (96) for the density is applicable down to zero temperature and provides the leading contribution in the small l_B limit. In the case of a one-dimensional potential $V(x)$, it is easy to check that the Gaussian integral over the coordinate Y in Eq. (96) leads to the expected Hermite polynomials. Regarding the remaining contributions that can be gathered from Eqs. (56) and (58), involving Landau mixing processes, a complete resummation scheme amounts to extra shifts in the energies, as discussed in Sec. III D. A final comparison is given in Fig. 2, which shows that, as long as $\omega_0 \ll \omega_c$, these improved quantum expressions are undistinguishable from the exact result.
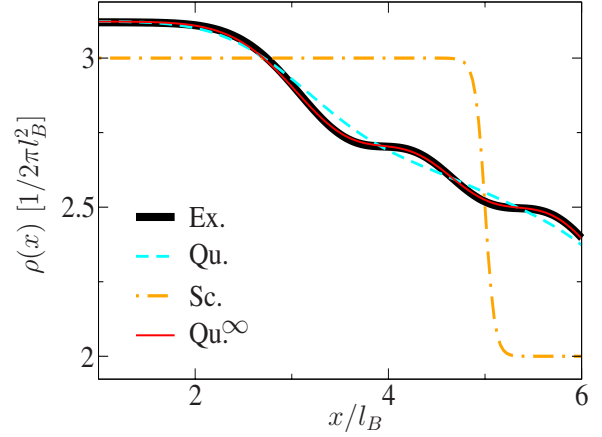

FIG. 2. (Color online) Local electronic density $\rho(x)$ for the same parameters as in Fig. 1(c), focusing on the compressible region between filling factors $n=2$ and $n=3$. This compares exact expression (81) (thick solid curve, label Ex.) undistinguishable from quantum expression (96) resummed to infinite order in l_B (thin solid curve, label Qu.$^\infty$), with semiclassical expansion (52) (dotted-dashed curve, label Sc.) and the quantum expansion up to order l_B^2 given by Eqs. (50), (56), and (58) (dashed curve, label Qu.).

VI. NONEQUILIBRIUM PROPERTIES

A. Distribution function and irreversibility

We have solved so far Hamiltonian (6) within the high magnetic-field expansion without fully specifying the potential-energy term $V(\mathbf{r})$. This scheme allows us to study the equilibrium and nonequilibrium situations on an equal footing. At equilibrium, $V(\mathbf{r})$ consists of a fixed background potential (including a confinement potential and an impurity random potential) and of a Hartree potential resulting from the mutual Coulomb interactions between the electrons. As a result of a self-consistent calculation, this yields a global effective electrostatic potential V_{eff} associated with local microscopic electric fields. In the nonequilibrium case, there is in addition an external potential-energy contribution reflecting the appearance of macroscopic electric fields and of macroscopic chemical-potential gradients in the system induced by the presence of a macroscopic current flow. Within the nonequilibrium regime, which is considered from now on in this section, the potential term $V(\mathbf{r})$ in Hamiltonian (6) consists thus of two different parts,

$$V(\mathbf{r}) = V_{\text{eff}}(\mathbf{r}) + e\Phi(\mathbf{r}). \qquad (98)$$

Here Φ is the nonequilibrium electrochemical potential that now varies in space. The latter term takes into account the presence of a macroscopic electromotive field $\mathbf{E} = -\boldsymbol{\nabla}_{\mathbf{r}}\Phi$.

In Ref. 35 we have solved the equation of motion for correlation Green's function $G^<$ in the vortex representation using the high magnetic-field expansion and have established that latter Green's function expressed in the vortex variables is related to the retarded and advanced Green's functions at any order of our expansion in the nonequilibrium stationary regime as

$$-iG^<_{\nu_1;\nu_2}(\omega) = in_F(\omega)[G^R_{\nu_1;\nu_2}(\omega) - G^A_{\nu_1;\nu_2}(\omega)]. \quad (99)$$

In the electronic representation, the quantity $-iG^<$ which has the character of a distribution function thus becomes

$$-iG^<(\mathbf{r},\mathbf{r}',\omega) = \sum_{\nu_1,\nu_2} \Psi^*_{\nu_2}(\mathbf{r}')\Psi_{\nu_1}(\mathbf{r})in_F(\omega)$$
$$\times [G^R_{\nu_1;\nu_2}(\omega) - G^A_{\nu_1;\nu_2}(\omega)], \quad (100)$$

where we have used Eq. (99). The fact that the same relation [Eq. (100)] holds in high magnetic fields in the equilibrium regime as well as in the nonequilibrium stationary regime can be understood as the realization of a local hydrodynamic equilibrium (or quasiequilibrium). This result, which has been established from the microscopic derivation of the quantum kinetic equation (see Ref. 35), is physically expected given that the microscopic characteristic length scale for the electron gas, namely, $l_B \propto B^{-1/2}$, becomes in high magnetic fields the shortest length scale. This means that it is possible to divide the system within a continuum description into elementary subsystems which are almost isolated from each other, permitting the introduction of thermodynamic variables depending on the space variable $\mathbf{r}$ (see, e.g., Ref. 39 and references therein).

It is worth mentioning that we have not introduced so far in the resolution of the Dyson equation any averaging to account for the presence of a random potential. In fact, this is not needed at this level since within the high magnetic-field expansion all the physics in the vortex representation appears to be purely local, the Hamiltonian being diagonalized in a closed-form order by order in powers of the magnetic length with the use of local vortex Green's functions $g_{m_1;m_2}(\mathbf{R})$. Dissipation and irreversibility, which are usually introduced already at the level of the Dyson equation with the impurity averaging procedure to account for the presence of random scattering interactions in zero or weak magnetic fields, take its roots within a different mechanism in high magnetic fields.

In fact, the stochastic character is intrinsic to our high magnetic-field expansion making use of the vortex basis, and we can associate somehow the transformation from the vortex to the electronic representations with a loss of information (thus irreversibility) provided that there exists some dynamical instability in the system. Indeed, by solving the Dyson equation in the vortex representation, we have basically augmented the set of allowed quantum states since the vortex basis is overcomplete. Note however that the expansion of the matrix elements of the potential in the vortex representation is granted in high fields due its unicity, which clearly results from the possibility to truncate the series expansion in the magnetic length l_B (see Ref. 35). Coming back to the electron representation, an indeterminacy illustrated by the presence of weight factors, namely, the wave functions $\Psi_\nu(\mathbf{r})$ in Eq. (100), appears, giving rise to a statistical-like description. Our high magnetic-field expansion alone contains thus microscopically the stochastic character which is a prerequisite ingredient for the expression of a loss of information. This loss becomes effective as soon as a dynamical instability associated with a divergence of neighboring trajectories exists in the system. This general view is corroborated by explicit calculations in the following. In Sec. VI C, we shall derive a microscopic expression for the conductivity tensor that is indeed associated in the nonequilibrium regime with an electrochemical potential drop occurring only in the vicinity of a local instability of the dynamics which, in the present case, is brought by the presence of saddle points of the local equilibrium density.

It is worth noting finally that we do not take into account the interaction of the system with an external environment. This alternative approach to dissipation considering the system plus reservoir couples the relevant quantum system to a large number of environmental degrees of freedom, such as phonons or quantum fluctuations of the electromagnetic field. Dissipation arises then because the system of interest can exchange energy with the rest of the larger system. More precisely, a loss of information is usually explicitly introduced in the calculations when tracing out these environmental degrees of freedom. We do not consider this mechanism of dissipation as being the most relevant here. On the contrary, the irreversibility mechanism described in this paper takes place in the bulk of the system itself, i.e., in the two-dimensional electron gas. This is a fundamental and key point in our transport theory. The relevance of a given approach to dissipation can finally be appreciated at the level of the comparison between theory and experiments, since the dissipative transport properties are strongly and intrinsically related to its dissipation mechanisms.

B. Nonequilibrium current density

Since the two potential-energy terms V_{eff} and $e\Phi$ in Eq. (98) can be treated technically on an equal footing in our high magnetic-field theory, the nonequilibrium current $\delta\mathbf{j}$ can, in fact, be rather straightforwardly deduced from the expressions of the equilibrium current density derived in Sec. IV and Appendix C.

The primary goal of this paper is not to provide a full quantitative analysis of macroscopic transport properties but just to show that our theory does contain information on microscopic dissipative mechanisms and thus allows us to fully determine the spatial dependence of the electrochemical potential $\Phi(\mathbf{r})$. For the sake of simplicity, we shall therefore restrict ourselves to the regime where the current density can be expressed in a local form [local expressions (73), (76), and (C11)–(C14)]. This regime does not correspond to the lowest temperatures for which the nonlocal nature of the current density associated with quantum tunneling becomes predominant.

It is clear, e.g., from formulas (73) and (76), that a nonequilibrium current can be generated in the linear response and at a uniform temperature by simultaneous density and electrostatic potential variations. This indicates that in principle we can separate the total current into two different contributions. One contribution corresponds to the diffusion current (terms involving gradients of the density) whose physical origin is associated with the tendency of the system to make the density uniform. The other contribution repre-

sents the current produced by the electric field which accelerates the electrons: it corresponds to electrical conduction which occurs by definition for a uniform density. The true driving force for the electrons is finally a combination of chemical and electrostatic potential differences, i.e., it is characterized by the variations of the electrochemical potential Φ which yield at the macroscopic scale a voltage drop. Although the roles of the electrostatic and chemical potentials are fundamentally different microscopically, the precise composition of Φ is irrelevant in the linear-response regime. Indeed, the integrated nonequilibrium electrical current can be seen, e.g., either as resulting entirely from a density-gradient current or equivalently as being entirely produced by macroscopic electrostatic variations (note that this equivalence is only valid in the linear response). In this paper, we shall adopt the point of view of the conduction mechanism, i.e., the case where a transport current $\delta\mathbf{j}$ is only sustained by electrostatic variations (the electrochemical potential changes are only identified with the electrostatic potential changes in the system).

Any analysis (semiclassical or quantum) of the nonequilibrium properties where interaction effects are expected to play a crucial role involves the simultaneous resolution of a transport equation and of the Poisson equation (in this direction, see, e.g., Ref. 29). Since the equilibrium and nonequilibrum regimes can be described with almost the same expressions, we can first consider at a qualitative level that the interaction effects in the nonequilibrium case do not differ substantially from that known in the equilibrium case. The screening in the compressible regions being almost perfect at low temperature, we expect *a priori* that the nonequilibrium conduction current is principally confined to the incompressible regions where most of the macroscopic electrostatic variations giving rise to voltage drops can occur (in other terms, this means that only one type of current—diffusion or conduction—contributes to a given region in the ideal case of perfect compressibility and incompressibility). This aspect concerning the nonequilibrium conduction current distribution has already been put forward by different authors.[29,30,40]

Using Eqs. (73), (76), (98), and (C11)–(C14) and keeping only the terms that are linear in variations of the electrochemical potential Φ (since we consider the linear response) and that do not contain derivatives of the Fermi function factor (we consider the conduction mechanism which involves the whole Fermi sea), we get at leading order for the nonequilibrium conduction current,

$$\delta\mathbf{j}_0(\mathbf{r}) = \frac{e^2}{h}\sum_{m=0}^{+\infty} n_F[\xi_m(\mathbf{r})]\boldsymbol{\nabla}_\mathbf{r}\Phi \times \hat{\mathbf{z}}. \tag{101}$$

From Eq. (77), we get a correcting contribution to the non-equilibrium current $\delta\mathbf{j}$ which is second order in l_B,

$$\delta\mathbf{j}_2(\mathbf{r}) = \frac{e^2}{h}\sum_{m=0}^{+\infty} n_F[\xi_m(\mathbf{r})]l_B^2\left[\frac{(\boldsymbol{\nabla}_\mathbf{r}\Phi\cdot\boldsymbol{\nabla}_\mathbf{r})}{\hbar\omega_c}\boldsymbol{\nabla}_\mathbf{r}V_{\text{eff}}\right.$$
$$\left.+\frac{(\boldsymbol{\nabla}_\mathbf{r}V_{\text{eff}}\cdot\boldsymbol{\nabla}_\mathbf{r})}{\hbar\omega_c}\boldsymbol{\nabla}_\mathbf{r}\Phi + \frac{3}{2}\left(m+\frac{1}{2}\right)\Delta_\mathbf{r}\boldsymbol{\nabla}_\mathbf{r}\Phi\right]\times\hat{\mathbf{z}}.$$
$$\tag{102}$$

From now on the Fermi factor $n_F[\xi_m(\mathbf{r})]$ is a functional of

the effective equilibrium potential V_{eff} which differs only slightly from the bare potential in the incompressible regions of the system where the screening is ineffective. A smooth spatial variation of the factor $n_F[\xi_m(\mathbf{r})]$ exists in these regions as a result of the finite temperature.

Obviously, leading contribution (101) yields local Ohm's law which takes the form

$$\delta\mathbf{j}_0(\mathbf{r}) = \hat{\sigma}(\mathbf{r})\mathbf{E}(\mathbf{r}) = \sigma_H(\mathbf{r})\hat{\mathbf{z}}\times\mathbf{E}(\mathbf{r}), \tag{103}$$

with a local conductivity tensor containing only the transverse Hall component,

$$\sigma_H(\mathbf{r}) = \frac{e^2}{h}\sum_{m=0}^{+\infty} n_F[\xi_m(\mathbf{r})], \tag{104}$$

where $\xi_m(\mathbf{r}) = E_m + V_{\text{eff}}(\mathbf{r})$. Ohm's law (103) with local Hall coefficient (104) is already well known and is used in most of the existing transport theories discussing the integer quantum Hall effect. The absence of diagonal components for the conductivity tensor in this (semiclassical) limit $l_B \to 0$ is rather welcome, since it is compatible with an extremely small longitudinal resistance as observed when the Hall resistance presents plateaus. However, this absence points out at the same time an insufficiency of formula (103) to describe the transition region between the Hall plateaus when high peaks of the longitudinal (dissipative) magnetoresistance are seen. This insufficiency is, in fact, cured when considering contribution (102) to the current arising from the next order terms in the l_B expansion, as shown further. At a general level, we note that our quantum-mechanical derivation of the transport current justifies on a microscopic basis the use of phenomenological models assuming a local conductivity tensor[28–33,41,42] that have been considered so far to explain successfully some transport features of the quantum Hall effect.

To our knowledge the first quantum corrections [Eq. (102)] to Ohm's law (103) had not been derived before in the literature. We find that they contain local corrections (which give rise to both transverse and diagonal components in the local conductivity tensor) as well as nonlocal corrections (terms involving second- and third-order derivatives of Φ). These nonlocal terms can be viewed as fingerprints of the nonlocal quantum tunneling processes in the considered semiclassical regime.

C. Spatial dependence of the electrochemical potential

The expansion of the current density in powers of l_B has led us quite naturally to a local continuum description of current conduction. Within this "classical" picture of transport (our theory is nevertheless developed in a fully quantum-mechanical framework), the stationary equation of continuity ensuring the charge conservation

$$\boldsymbol{\nabla}_\mathbf{r}\cdot\mathbf{j} = 0, \tag{105}$$

supplemented by boundary conditions, constrains the spatial dependence of the electrochemical potential when applied to

the nonequilibrium current density $\delta\mathbf{j}$ provided that some dissipation mechanisms are accounted for within the considered expressions for $\delta\mathbf{j}$ [note that Eq. (105) becomes an identity for the equilibrium current density, as can be easily checked].

Inserting the leading contribution $\delta\mathbf{j}_0$ [Eq. (103)] into Eq. (105) and using $\mathbf{E}=-\boldsymbol{\nabla}_{\mathbf{r}}\Phi$, we get the equation

$$(\boldsymbol{\nabla}_{\mathbf{r}}\sigma_H \times \boldsymbol{\nabla}_{\mathbf{r}}\Phi) \cdot \hat{\mathbf{z}} = 0, \tag{106}$$

which has been thoroughly discussed in the literature.[28,31,32] From this equation, it turns out that the electrochemical potential lines and the lines of constant σ_H must coincide. It is worth noting that condition (106) is automatically obeyed at the critical points of σ_H which correspond also to the critical points of the density or of the potential V_{eff}. This means that there still exists a degeneracy in the vicinity of these critical points, which has to be lifted. Although being small, the correcting contributions [Eq. (102)] will play this important role of dictating locally the spatial dependence of $\Phi(\mathbf{r})$, as we prove now.

Since we are considering the nonequilibrium current density in the neighborhood of $\boldsymbol{\nabla}_{\mathbf{r}}V_{\text{eff}}=0$, we can first safely ignore in Eq. (102) the term proportional to $\boldsymbol{\nabla}_{\mathbf{r}}V_{\text{eff}}$ and which involves the second-order derivative of Φ. At a preliminary stage, we shall also disregard the other nonlocal term (with the third-order derivative of Φ) and justify this assumption *a posteriori*. Consequently, the second-order contribution to the current reduces to

$$\delta\mathbf{j}_2(\mathbf{r}) \approx \frac{e^2}{h}\sum_{m=0}^{+\infty} n_F[\xi_m(\mathbf{r})]l_B^2 \frac{(\boldsymbol{\nabla}_{\mathbf{r}}\Phi \cdot \boldsymbol{\nabla}_{\mathbf{r}})}{\hbar\omega_c}\boldsymbol{\nabla}_{\mathbf{r}}V_{\text{eff}} \times \hat{\mathbf{z}}. \tag{107}$$

Combining this Eq. (107) with Eq. (103), we get local Ohm's law with a local conductivity tensor being given by

$$\hat{\sigma}(\mathbf{r}) = \sigma_H(\mathbf{r})\begin{pmatrix} 0 & -1 \\ 1 & 0 \end{pmatrix}\left(\hat{1} + \frac{l_B^2}{\hbar\omega_c}\hat{\mathcal{H}}[V_{\text{eff}}](\mathbf{r})\right), \tag{108}$$

where $\hat{1}$ is the 2×2 identity matrix and $\hat{\mathcal{H}}$ is the Hessian matrix of the function V_{eff}, i.e., we have $\hat{\mathcal{H}}[V_{\text{eff}}]_{ij}(\mathbf{r})=\partial_{ij}^2 V_{\text{eff}}(\mathbf{r})$.

We remark that the local conductivity tensor does not exhibit the usual symmetries, i.e., the Onsager-Casimir reciprocity relations. For example, we find here that generally $\sigma_{xx}(\mathbf{r})=-\sigma_{yy}(\mathbf{r})$ and $\sigma_{xy}(\mathbf{r}) \neq -\sigma_{yx}(\mathbf{r})$, whereas the Onsager relations imply $\sigma_{xx}=\sigma_{yy}$ and $\sigma_{xy}=-\sigma_{yx}$. In fact, it is worth noting that the Onsager relations result from fingerprints of the time-reversal invariance of the microscopic equations after some averaging procedure (see, e.g., Ref. 39). In the present case, we have derived a local conductivity tensor from the microscopic equations without resorting to any averaging procedure. Obviously, the local terms involving the Hessian matrix contribution vanish in the volume average; the Onsager relations are then restored. This indicates that the Hessian matrix terms can be interpreted as a

result of *local fluctuations* only. Let us also emphasize that current (107) purely stems from Landau level mixing processes. The found sign difference between the two local diagonal components which appears as rather unexpected and unconventional could be seen as a reminiscence of the antisymmetry imposed by the Lorentz force, antisymmetry which is usually only exhibited by the Hall components (see the conductivity tensor at leading order). Anyway, we shall show in the following that the precise form we have found for the local conductivity tensor leads to reliable physical results.

Inserting second-order contribution (107) into the continuity equation [Eq. (105)], condition (106) is now replaced by the differential equation,

$$(\boldsymbol{\nabla}_{\mathbf{r}}\sigma_H \times \boldsymbol{\nabla}_{\mathbf{r}}\Phi) \cdot \hat{\mathbf{z}} - \frac{l_B^2}{\hbar\omega_c}\sigma_H \operatorname{Tr}\left\{\begin{pmatrix} 0 & -1 \\ 1 & 0 \end{pmatrix}\hat{\mathcal{H}}[V_{\text{eff}}]\hat{\mathcal{H}}[\Phi]\right\}$$
$$= 0, \tag{109}$$

where the notation Tr means the trace. In the neighborhood of a critical point, which for practical convenience is taken at the origin ($x=y=0$), we have

$$\boldsymbol{\nabla}_{\mathbf{r}}\sigma_H(\mathbf{r}) \approx (\mathbf{r}\cdot\boldsymbol{\nabla}_{\mathbf{r}})\boldsymbol{\nabla}_{\mathbf{r}}\sigma_H|_0. \tag{110}$$

The Hessian matrices of the function $\sigma_H(\mathbf{r})$ and of the function $V_{\text{eff}}(\mathbf{r})$ being proportional at the critical point, we can choose, without loss of generality according to the form of Eq. (109), the $\hat{\mathbf{x}}$ and $\hat{\mathbf{y}}$ axes such that both Hessian matrices are diagonal. This means, e.g., that $V_{\text{eff}}(\mathbf{r})$ is expanded close to the origin as

$$V_{\text{eff}}(\mathbf{r}) = V_{\text{eff}}(0) + a\frac{x^2}{2} + b\frac{y^2}{2}, \tag{111}$$

where $a=\partial_{xx}^2 V_{\text{eff}}|_0$ and $b=\partial_{yy}^2 V_{\text{eff}}|_0$. For this situation, Eq. (109) becomes then

$$(a-b)\partial_{xy}^2\Phi + \frac{1}{\lambda^2}[ax\partial_y\Phi - by\partial_x\Phi] = 0, \tag{112}$$

with

$$\lambda^2 = l_B^2 \frac{\displaystyle\sum_{m=0}^{+\infty} n_F[\xi_m(0)]}{\displaystyle\sum_{m=0}^{+\infty} \hbar\omega_c\{-n_F'[\xi_m(0)]\}}. \tag{113}$$

To get rid of coefficients a and b in the differential equation [Eq. (112)], it is useful to introduce the change in variables,

$$x' = \alpha x - \beta y, \tag{114}$$

$$y' = \alpha x + \beta y. \tag{115}$$

If the critical point corresponds to a local extremum (situation with $ab>0$), we can take

$$\alpha = \sqrt{\left|\frac{a}{a-b}\right|}, \quad \beta = \sqrt{\left|\frac{b}{a-b}\right|}, \quad (116)$$

and Eq. (112) then reduces to

$$\partial^2_{y'y'}\Phi - \partial^2_{x'x'}\Phi + \frac{\epsilon}{\lambda^2}[x'\partial_{y'}\Phi - y'\partial_{x'}\Phi] = 0, \quad (117)$$

where $\epsilon = +1$ if $|a| > |b|$ and $\epsilon = -1$ if $|a| < |b|$. The general solution of Eq. (117) is

$$\Phi(x',y') = [A + Be^{-\epsilon x'y'/\lambda^2}][C + D(x'^2 + y'^2)], \quad (118)$$

where the coefficients A, B, C, and D are constants of integration. As boundary conditions, we require that the electrochemical potential tends to constant values far from the critical point. We therefore necessarily get $D = B = 0$. There is consequently no macroscopic voltage drop associated with the crossing of a local extremum (the special case $a = b \neq 0$, which can be readily obtained from Eq. (112) leads to the same result).

Now, if the critical point corresponds to a saddle-point (situation with $ab < 0$), we can choose

$$\alpha = \sqrt{\frac{a}{a-b}}, \quad \beta = \sqrt{\frac{b}{b-a}}, \quad (119)$$

so that Eq. (112) becomes

$$\partial^2_{y'y'}\Phi - \partial^2_{x'x'}\Phi + \frac{1}{\lambda^2}[y'\partial_{y'}\Phi - x'\partial_{x'}\Phi] = 0. \quad (120)$$

Looking for a solution with separable spatial dependences, we find that the only solution of Eq. (120) represents the product of two error step functions in the x' and y' directions,

$$\Phi(x',y') = \left[A + B \, \mathrm{erf}\left(\frac{x'}{\sqrt{2}\lambda}\right)\right]\left[C + D \, \mathrm{erf}\left(\frac{y'}{\sqrt{2}\lambda}\right)\right], \quad (121)$$

where

$$\mathrm{erf}(x) = \frac{2}{\sqrt{\pi}}\int_0^x e^{-t^2}dt. \quad (122)$$

We observe with solution (121) that far from the saddle point the electrochemical potential tends to different constant values depending on sectors. This solution is consistent with the picture of four different regions characterized by four different electrochemical potential values with an electrochemical drop resulting from the saddle-point crossing, which is a major ingredient in the network models that have been developed to describe the peaks of the longitudinal conductance in the transition regime between quantized Hall plateaus (see, e.g., Ref. 41). Thus, our conductivity tensor confirms at a microscopic level the special role played by the saddle points of the density in the dissipative features.[17,28,37,41,43,44]

Finally, we turn back to the condition of validity of Eq. (109) which has been established under the assumption that the nonlocal term in Eq. (102) involving the third-order derivatives of Φ plays a negligible role. Clearly, this is justified provided that Φ is smooth enough. Considering expression (113) giving the characteristic length scale λ for the spatial variations of the electrochemical potential, we note that this assumption appears fully justified as long as the function $n'_F[\xi_m(0)]$ remains quite small, i.e., as long as the saddle-point filling factor is close to an integer. Conversely, we can conclude that the nonlocal term which is associated with quantum tunneling becomes non-negligible at low temperatures when the local chemical potential $\mu(0) = \mu^* - V_{\mathrm{eff}}(0)$ approaches a Landau level. This regime which occurs for a narrow range in magnetic fields will be investigated in detail elsewhere.

VII. CONCLUSION AND PERSPECTIVES

A. Summary

In summary, we have developed a systematic high magnetic-field expansion, which permits to find in a recursive way, order by order in powers of the magnetic length l_B, Green's functions for the quantum problem of an electron confined to a plane and subjected to a slowly varying potential in high magnetic fields. Using this theory, we have derived functional quantum expressions for the local equilibrium density distribution and current density at the first two leading orders. These expressions which contain Landau level mixing processes in a controlled way and quantum smearing effects associated with the finite extent of the wave function at finite magnetic fields form the starting point for future quantitative investigations of screening effects at low temperatures in two-dimensional disordered Hall liquids. We have checked the accuracy of our general functionals against the exact solution of a one-dimensional parabolic confining potential, demonstrating the controlled character of the theory to get equilibrium properties. Furthermore, we have shown that our technique gives a natural and systematic access to semiclassical expansions in powers of the magnetic length of the physical observables. For example, we have been able to derive the semiclassical corrections of order l_B^2 for the local charge and current densities.

Moreover, we have proved microscopically that in high magnetic fields the electronic system can be described within a local hydrodynamic regime and that the electrical conduction transport takes a quasilocal form. As an important result, we have put forward that our approximation scheme with the l_B expansion intrinsically captures dissipation mechanisms at the microscopic level and accounts for quantum tunneling processes. For example, we have derived microscopic expressions for the local conductivity tensor, which contains both Hall and longitudinal components, the dissipative features appearing at the order l_B^2, i.e., at finite magnetic fields. Furthermore, we have established from the special form of this local conductivity tensor that a nonzero gradient of the electrochemical potential is exclusively generated by the saddle points of the density distribution. A general understanding of the transport properties at the microscopic level now seems accessible. However, the procedure of computation of the macroscopic transport coefficients, and in particu-

lar the treatment of nonlocal effects induced by quantum tunneling, requires additional work that is currently underway.

B. General perspective

Finally, we want to address a more general perspective, which is beyond the quantum Hall effect, namely, the issue of dissipation in physics and especially in quantum mechanics. Indeed, we believe that our systematic expansion in ascending powers of the magnetic length could shed light on this important issue by illustrating how the irreversible evolution of a quantum system can emerge from the consideration of microscopic equations which are time-reversal invariant. The system considered in this paper is maybe the simplest system one can consider to answer the latter question, since it involves only 2 degrees of freedom. Interestingly, the magnetic field (which plays the role of a tuning parameter here) controls the degree of mixing between these 2 degrees of freedom, which corresponds at the classical level to the cyclotron motion and the guiding-center motion. In high magnetic fields and for a smooth arbitrary potential, this mixing becomes very weak as a result of the strongly different time scales associated with the two kinds of motion. The system even becomes dynamically integrable in the strict limit of infinite magnetic fields when the mixing between the 2 degrees of freedom is no more possible. Therefore, the high but finite magnetic-field regime can be associated with a classical regime of soft chaos. At the quantum-mechanical level, it is clear that the quantization of the kinetic orbital motion which introduces robustness (in the sense that it considerably constrains the possible variations of the orbital motion) renders this exchange between the 2 degrees of freedom even much more ineffective. We thus expect that the quantum system is somehow even closer to integrability than the classical one.

In classical chaotic systems (this is, for example, the case for the present disordered system in low magnetic fields), irreversibility and dissipation are often associated with the technical impossibility to fully describe the trajectories as a result of complicated mixing mechanisms between the degrees of freedom. This complexity is then transposed in terms of a stochastic description, thus expressing a loss of information. We have shown that in high magnetic fields it is not required to average over the disorder configuration in order to find an analytical approximate solution to the quantum problem, contrary to the situation at low magnetic fields. Moreover, we have noticed that time irreversibility has nevertheless been introduced at some stage of the derivation, since our high magnetic-field theory accounts for dissipation features related to time-decaying states. It turns out from first considerations that the dissipation involves Landau level mixing processes and arises from the conjunction of local quantum fluctuations with a local dynamical instability taking place at the saddle points of the local equilibrium density (a saddle point is necessarily characterized by stable and unstable directions which can be defined in an obvious manner). Interestingly, in low magnetic fields the electrical conduction is also directly related to another insta-

bility mechanism which is realized by the sensitivity to the initial condition characterizing the chaotic systems. In brief, insights in this general perspective of understanding the emergence of dissipation in quantum-mechanical systems could be gained from closer investigations of the high magnetic-field expansion developed in the present work.

APPENDIX A: OFF-DIAGONAL ELEMENTS OF THIRD-ORDER GREEN'S FUNCTIONS

In this Appendix, we provide the detail for the derivation of the elements $\delta_{m_1,m_2\pm1}$ of third-order Green's function $g^{(3)}$, which are needed for the computation of the second-order current density performed in Sec. IV and Appendix C. The function $g^{(3)}$ obeys the equation

$$
\begin{aligned}
\omega_{m_1} g^{(3)}_{m_1;m_2}(\mathbf{R}) &= v^{(3)}_{m_1;m_2}(\mathbf{R}) g^{(0)}_{m_2;m_2}(\mathbf{R}) + \sum_{m_3} \left[v^{(2)}_{m_1;m_3}(\mathbf{R}) g^{(1)}_{m_3;m_2}(\mathbf{R}) \right. \\
&\quad \left. + v^{(1)}_{m_1;m_3}(\mathbf{R}) g^{(2)}_{m_3;m_2}(\mathbf{R}) \right] + (\partial_X - i\partial_Y) V(\mathbf{R}) \\
&\quad \times (\partial_X + i\partial_Y) g^{(1)}_{m_1;m_2}(\mathbf{R}) + (\partial_X - i\partial_Y) v^{(1)}_{m_1;m_2}(\mathbf{R}) \\
&\quad \times (\partial_X + i\partial_Y) g^{(0)}_{m_2;m_2}(\mathbf{R}).
\end{aligned}
\tag{A1}
$$

Here is a list of these numerous components $\delta_{m_1,m_2\pm1}$ of $g^{(3)}_{m_1;m_2}(\mathbf{R})$ arising (i) from the combination $v^{(3)}g^{(0)}$,

$$
\begin{aligned}
\frac{1}{2\omega_{m_1}\omega_{m_2}} &[(m_1+1)\sqrt{m_1}\,\delta_{m_1,m_2+1}(\partial_X - i\partial_Y) \\
&+ (m_2+1)\sqrt{m_2}\,\delta_{m_1+1,m_2}(\partial_X + i\partial_Y)]\Delta V,
\end{aligned}
\tag{A2}
$$

(ii) from the combination $v^{(2)}g^{(1)}$,

$$
\begin{aligned}
\frac{m_1+1}{\omega_{m_1}^2 \omega_{m_2}} &\Delta_{\mathbf{R}} V [\sqrt{m_1}\,\delta_{m_1,m_2+1}(\partial_X - i\partial_Y) \\
&+ \sqrt{m_2}\,\delta_{m_1+1,m_2}(\partial_X + i\partial_Y)]V \\
&+ \frac{m_2\sqrt{m_1}}{2\omega_{m_2-1}\omega_{m_2}\omega_{m_2+1}} \delta_{m_1,m_2+1}[(\partial_X - i\partial_Y)^2 V](\partial_X + i\partial_Y)V \\
&+ \frac{(m_2+1)\sqrt{m_2}}{2\omega_{m_2-1}\omega_{m_2}\omega_{m_2+1}} \delta_{m_1+1,m_2}[(\partial_X + i\partial_Y)^2 V](\partial_X - i\partial_Y)V,
\end{aligned}
\tag{A3}
$$

(iii) from the combination $v^{(1)}g^{(2)}$,

$$\frac{m_2+1}{\omega_{m_1}\omega_{m_2}^2}\Delta_{\mathbf{R}}V[\sqrt{m_1}\delta_{m_1,m_2+1}(\partial_X-i\partial_Y)+\sqrt{m_2}\delta_{m_1+1,m_2}(\partial_X+i\partial_Y)]V+\left[\frac{m_2+1}{\omega_{m_2+1}}+\frac{m_2}{\omega_{m_2-1}}+\frac{1}{\omega_{m_2}}\right]\frac{|\nabla_{\mathbf{R}}V|^2}{\omega_{m_2}^2\omega_{m_1}}$$

$$\times[\sqrt{m_1}\delta_{m_1,m_2+1}(\partial_X-i\partial_Y)+\sqrt{m_2}\delta_{m_1+1,m_2}(\partial_X+i\partial_Y)]V+\frac{m_1\sqrt{m_2}}{2\omega_{m_1-1}\omega_{m_1}\omega_{m_1+1}}\delta_{m_1+1,m_2}[(\partial_X-i\partial_Y)V][(\partial_X+i\partial_Y)^2V]$$

$$+\frac{(m_1+1)\sqrt{m_1}}{2\omega_{m_1-1}\omega_{m_1}\omega_{m_1+1}}\delta_{m_1,m_2+1}[(\partial_X+i\partial_Y)V][(\partial_X-i\partial_Y)^2V]+\frac{m_1\sqrt{m_2}}{\omega_{m_1-1}\omega_{m_1}^2\omega_{m_1+1}}\delta_{m_1+1,m_2}[(\partial_X-i\partial_Y)V][(\partial_X+i\partial_Y)V]^2$$

$$+\frac{(m_1+1)\sqrt{m_1}}{\omega_{m_1-1}\omega_{m_1}^2\omega_{m_1+1}}\delta_{m_1,m_2+1}[(\partial_X+i\partial_Y)V][(\partial_X-i\partial_Y)V]^2, \tag{A4}$$

and (iv) from the combinations $(\partial_X-i\partial_Y)v(\partial_X+i\partial_Y)g$,

$$|\nabla_{\mathbf{R}}V|^2\left[\frac{1}{\omega_{m_1}^3\omega_{m_2}}+\frac{1}{\omega_{m_1}^2\omega_{m_2}^2}\right][\sqrt{m_1}(\partial_X-i\partial_Y)\delta_{m_1,m_2+1}+\sqrt{m_2}(\partial_X+i\partial_Y)\delta_{m_1+1,m_2}]V+\frac{\Delta_{\mathbf{R}}V}{\omega_{m_1}\omega_{m_2}}\left[\frac{\sqrt{m_1}}{\omega_{m_1}}(\partial_X-i\partial_Y)\delta_{m_1,m_2+1}\right.$$

$$\left.+\frac{\sqrt{m_2}}{\omega_{m_2}}(\partial_X+i\partial_Y)\delta_{m_1+1,m_2}\right]V+\frac{\sqrt{m_1}}{\omega_{m_1}\omega_{m_2}^2}\delta_{m_1,m_2+1}[(\partial_X-i\partial_Y)^2V][(\partial_X+i\partial_Y)V]+\frac{\sqrt{m_2}}{\omega_{m_1}^2\omega_{m_2}}\delta_{m_1+1,m_2}[(\partial_X+i\partial_Y)^2V][(\partial_X-i\partial_Y)V]. \tag{A5}$$

Regrouping the terms of the same form, different contributions (A2)–(A5) to the components $\delta_{m_1,m_2\pm1}$ of $g^{(3)}$ are rearranged as (i) terms with $\Delta_{\mathbf{R}}(\partial_X\pm i\partial_Y)V$,

$$\frac{1}{2}\Delta_{\mathbf{R}}[(m_1+1)\sqrt{m_1}\delta_{m_1,m_2+1}(\partial_X-i\partial_Y)+(m_2+1)\sqrt{m_2}\delta_{m_1+1,m_2}(\partial_X+i\partial_Y)]V/\omega_{m_1}\omega_{m_2}, \tag{A6}$$

(ii) terms with $\Delta_{\mathbf{R}}V(\partial_X\pm i\partial_Y)V$,

$$\Delta_{\mathbf{R}}V\left[\frac{m_2+1}{\omega_{m_1}\omega_{m_2}^2}+\frac{m_1+1}{\omega_{m_2}\omega_{m_1}^2}\right][\sqrt{m_1}\delta_{m_1,m_2+1}(\partial_X-i\partial_Y)+\sqrt{m_2}\delta_{m_1+1,m_2}(\partial_X+i\partial_Y)]V+\frac{\Delta_{\mathbf{R}}V}{\omega_{m_1}\omega_{m_2}}\left[\frac{\sqrt{m_1}}{\omega_{m_1}}(\partial_X-i\partial_Y)\delta_{m_1,m_2+1}\right.$$

$$\left.+\frac{\sqrt{m_2}}{\omega_{m_2}}(\partial_X+i\partial_Y)\delta_{m_1+1,m_2}\right]V, \tag{A7}$$

(iii) terms with $[(\partial_X\pm i\partial_Y)^2V](\partial_X\mp i\partial_Y)V$,

$$\frac{1}{2}\left\{\left[\frac{m_2}{\omega_{m_2-1}\omega_{m_2}\omega_{m_2+1}}+\frac{m_1+1}{\omega_{m_1-1}\omega_{m_1}\omega_{m_1+1}}+\frac{2}{\omega_{m_1}\omega_{m_2}^2}\right]\sqrt{m_1}\delta_{m_1,m_2+1}[(\partial_X-i\partial_Y)^2V][(\partial_X+i\partial_Y)V]\right.$$

$$\left.+\left[\frac{m_1}{\omega_{m_1-1}\omega_{m_1}\omega_{m_1+1}}+\frac{m_2+1}{\omega_{m_2-1}\omega_{m_2}\omega_{m_2+1}}+\frac{2}{\omega_{m_1}^2\omega_{m_2}}\right]\sqrt{m_2}\delta_{m_1+1,m_2}[(\partial_X+i\partial_Y)^2V][(\partial_X-i\partial_Y)V]\right\}, \tag{A8}$$

and (iv) terms with $|\nabla_{\mathbf{R}}V|^2(\partial_X\pm i\partial_Y)V$,

$$\frac{|\nabla_{\mathbf{R}}V|^2}{\omega_{m_1}\omega_{m_2}}\left\{\left[\frac{m_1+1}{\omega_{m_1}\omega_{m_1+1}}+\frac{m_2}{\omega_{m_2-1}\omega_{m_2}}+\frac{m_1+1}{\omega_{m_1}\omega_{m_2}}+\frac{1}{\omega_{m_1}^2}+\frac{1}{\omega_{m_2}^2}\right]\sqrt{m_1}\delta_{m_1,m_2+1}[(\partial_X-i\partial_Y)V]\right.$$

$$\left.+\left[\frac{m_2+1}{\omega_{m_2}\omega_{m_2+1}}+\frac{m_1}{\omega_{m_1-1}\omega_{m_1}}+\frac{m_2+1}{\omega_{m_1}\omega_{m_2}}+\frac{1}{\omega_{m_1}^2}+\frac{1}{\omega_{m_2}^2}\right]\sqrt{m_2}\delta_{m_1+1,m_2}[(\partial_X+i\partial_Y)V]\right\}. \tag{A9}$$

APPENDIX B: PROOF OF USEFUL RELATIONS

In this appendix we prove identities (54), (C1), and (C2). First, with the help of Eq. (69) we can find that

$$(\partial_x - i\partial_y)|\Psi_{p,\mathbf{R}}(\mathbf{r})|^2 = \frac{\sqrt{2}}{l_B}[\sqrt{p}\Psi_{p,\mathbf{R}}^*(\mathbf{r})\Psi_{p-1,\mathbf{R}}(\mathbf{r}) - \sqrt{p+1}\Psi_{p+1,\mathbf{R}}^*(\mathbf{r})\Psi_{p,\mathbf{R}}(\mathbf{r})], \quad \text{(B1)}$$

which defines in a recursive way the combination $\sqrt{p+1}\Psi_{p+1,\mathbf{R}}^*(\mathbf{r})\Psi_{p,\mathbf{R}}(\mathbf{r})$. From this relation (B1), it is then straightforward to obtain identity (54).

Using Eq. (69), it can be readily established that

$$(\partial_x - i\partial_y)\{\Psi_{m,\mathbf{R}}(\mathbf{r})\Psi_{m+1,\mathbf{R}}^*(\mathbf{r})\} = \frac{\sqrt{2}}{l_B}[\sqrt{m}\Psi_{m-1,\mathbf{R}}(\mathbf{r})\Psi_{m+1,\mathbf{R}}^*(\mathbf{r}) - \sqrt{m+2}\Psi_{m,\mathbf{R}}(\mathbf{r})\Psi_{m+2,\mathbf{R}}^*(\mathbf{r})]. \quad \text{(B2)}$$

From this relation (B2), we deduce that

$$\sqrt{m+2}\Psi_{m+2,\mathbf{R}}^*(\mathbf{r})\Psi_{m,\mathbf{R}}(\mathbf{r}) = \sqrt{m}\Psi_{m+1,\mathbf{R}}^*(\mathbf{r})\Psi_{m-1,\mathbf{R}}(\mathbf{r}) - \frac{l_B}{\sqrt{2}}(\partial_x - i\partial_y) \times \{\Psi_{m+1,\mathbf{R}}^*(\mathbf{r})\Psi_{m,\mathbf{R}}(\mathbf{r})\}. \quad \text{(B3)}$$

Multiplying Eq. (B3) by $\sqrt{m+1}$, we get a recursive relation which yields

$$\sqrt{m+1}\sqrt{m+2}\Psi_{m+2,\mathbf{R}}^*(\mathbf{r})\Psi_{m,\mathbf{R}}(\mathbf{r})$$
$$= -\frac{l_B}{\sqrt{2}}(\partial_x - i\partial_y)\sum_{p=0}^{m}\sqrt{p+1}\Psi_{p+1,\mathbf{R}}^*(\mathbf{r})\Psi_{p,\mathbf{R}}(\mathbf{r}). \quad \text{(B4)}$$

Finally, using identity (54), we get the result [Eq. (C1)].

From Eq. (69), we can get

$$\Delta_{\mathbf{r}}|\Psi_{p,\mathbf{R}}(\mathbf{r})|^2 = \frac{2}{l_B^2}\{(p+1)|\Psi_{p+1,\mathbf{R}}(\mathbf{r})|^2 + p|\Psi_{p-1,\mathbf{R}}(\mathbf{r})|^2 - (2p+1)|\Psi_{p,\mathbf{R}}(\mathbf{r})|^2\}. \quad \text{(B5)}$$

Therefore, we can write

$$\sum_{p=0}^{m}(m+1-p)\Delta_{\mathbf{r}}|\Psi_{p,\mathbf{R}}(\mathbf{r})|^2 = \frac{2}{l_B^2}\sum_{p=0}^{m}(m+1-p)\{(p+1) \times |\Psi_{p+1,\mathbf{R}}(\mathbf{r})|^2 + p|\Psi_{p-1,\mathbf{R}}(\mathbf{r})|^2 - (2p+1)|\Psi_{p,\mathbf{R}}(\mathbf{r})|^2\}$$
$$= \frac{2}{l_B^2}((m+1)|\Psi_{m+1,\mathbf{R}}(\mathbf{r})|^2 - \sum_{p=0}^{m}|\Psi_{p,\mathbf{R}}(\mathbf{r})|^2), \quad \text{(B6)}$$

which proves identity (C2).

APPENDIX C: CALCULATION OF THE ELECTRONIC CURRENT AT ORDER l_B^2

In this appendix we present the detailed derivation of the quantum (Appendix C 1) and semiclassical (Appendix C 2) expressions for the electronic current density up to order l_B^2.

1. Quantum expressions for the current

a. Contribution from $g^{(1)}$

First-order vortex Green's function has the total contribution to the current given by formula (74), from which the leading-order term was extracted in Eq. (75). We express here formula (74) in a form that makes explicit its leading and subdominant contributions. Using the identities proven in Appendix B

$$\sqrt{m+1}\sqrt{m+2}\Psi_{m+2,\mathbf{R}}^*(\mathbf{r})\Psi_{m,\mathbf{R}}(\mathbf{r}) = \left[-\frac{l_B}{\sqrt{2}}(\partial_x - i\partial_y)\right]^2 \times \sum_{p=0}^{m}(m+1-p)|\Psi_{p,\mathbf{R}}(\mathbf{r})|^2, \quad \text{(C1)}$$

$$\frac{l_B^2}{2}\Delta_{\mathbf{r}}\sum_{p=0}^{m}(m+1-p)|\Psi_{p,\mathbf{R}}(\mathbf{r})|^2 = (m+1)|\Psi_{m+1,\mathbf{R}}(\mathbf{r})|^2 - \sum_{p=0}^{m}|\Psi_{p,\mathbf{R}}(\mathbf{r})|^2, \quad \text{(C2)}$$

we can rewrite the combination $\Psi_{m,\mathbf{R}}(\mathbf{r})\Psi_{m+2,\mathbf{R}}^*(\mathbf{r})$ of vortex wave functions appearing in Eq. (74) in the following way:

$$\sqrt{m+1}\sqrt{m+2}\binom{\text{Im}}{\text{Re}}(\partial_X V + i\partial_Y V)\Psi_{m,\mathbf{R}}(\mathbf{r})\Psi_{m+2,\mathbf{R}}^*(\mathbf{r})$$
$$= l_B^2\hat{\mathbf{z}} \times (\boldsymbol{\nabla}_{\mathbf{R}} V \cdot \boldsymbol{\nabla}_{\mathbf{r}})\boldsymbol{\nabla}_{\mathbf{r}}\sum_{p=0}^{m}(m+1-p)|\Psi_{p,\mathbf{R}}(\mathbf{r})|^2$$
$$+ \hat{\mathbf{z}} \times \boldsymbol{\nabla}_{\mathbf{R}} V(\sum_{p=0}^{m}|\Psi_{p,\mathbf{R}}(\mathbf{r})|^2 - (m+1)|\Psi_{m+1,\mathbf{R}}(\mathbf{r})|^2). \quad \text{(C3)}$$

Inserting expressions (55) and (C3) in Eq. (74), we then express the current density as

$$\mathbf{j}^{(1)}(\mathbf{r}) = \frac{e\hbar}{m^*}\int\frac{d^2\mathbf{R}}{2\pi l_B^2}\sum_{m=0}^{+\infty}\frac{n_F[\xi_{m+1}(\mathbf{R})] - n_F[\xi_m(\mathbf{R})]}{\hbar\omega_c}$$
$$\times(\sum_{p=0}^{m}|\Psi_{p,\mathbf{R}}(\mathbf{r})|^2\hat{\mathbf{z}} \times \boldsymbol{\nabla}_{\mathbf{R}} V(\mathbf{R})$$
$$+ l_B^2\hat{\mathbf{z}} \times [\boldsymbol{\nabla}_{\mathbf{R}} V(\mathbf{R}) \cdot \boldsymbol{\nabla}_{\mathbf{r}}]\boldsymbol{\nabla}_{\mathbf{r}}\sum_{p=0}^{m}(m+1/2-p)|\Psi_{p,\mathbf{R}}(\mathbf{r})|^2), \quad \text{(C4)}$$

where we have used

$$\nabla_{\mathbf{r}}(\nabla_{\mathbf{R}}V \cdot \nabla_{\mathbf{r}}|\Psi_{p,\mathbf{R}}(\mathbf{r})|^2) = [\nabla_{\mathbf{R}}V \cdot \nabla_{\mathbf{r}}]\nabla_{\mathbf{r}}(|\Psi_{p,\mathbf{R}}(\mathbf{r})|^2).$$
(C5)

After a straightforward simplification of expression (C4), the current density $\mathbf{j}^{(1)}$ can finally be divided into a leading contribution given by Eq. (75) and a subdominant contribution which reads

$$\mathbf{j}_{\text{sub}}^{(1)}(\mathbf{r}) = \frac{e}{h}\int d^2\mathbf{R} \sum_{m=0}^{+\infty} n_F[\xi_m(\mathbf{R})]l_B^2$$

$$\times [\nabla_{\mathbf{R}}V(\mathbf{R}) \cdot \nabla_{\mathbf{r}}]\nabla_{\mathbf{r}}\left(\sum_{p=0}^{m}|\Psi_{p,\mathbf{R}}(\mathbf{r})|^2 - \frac{|\Psi_{m,\mathbf{R}}(\mathbf{r})|^2}{2}\right) \times \hat{\mathbf{z}}.$$
(C6)

b. Contribution from $g^{(2)}$

Second-order vortex Green's function (35) contains diagonal elements ($m=m'$), which contribute within the first and second terms in the right-hand side of Eq. (71). It has also

off-diagonal elements $\delta_{m,m'\pm 2}$, which combine with the second term of the right-hand side of Eq. (71), to give terms involving wave functions with adjacent Landau levels (wave functions with a Landau index difference of 3 are also obtained, but these contribute to the current at order l_B^4 and will be discarded). After inspection, the contribution from the function $g^{(0)}$ appearing with the term $k=1$ in Eq. (71) combines very naturally with these terms from $g^{(2)}$, so that the starting expression reads

$$\mathbf{j}^{(2)}(\mathbf{r}) = \frac{e\hbar}{2m^*}\hat{\mathbf{z}} \times \nabla_{\mathbf{r}}\rho^{(2)}(\mathbf{r}) + \frac{e\hbar}{m^*}\int\frac{d\omega}{2\pi}\int\frac{d^2\mathbf{R}}{2\pi l_B^2}\sum_{m=0}^{+\infty}\frac{l_B}{\sqrt{2}}\sqrt{m+1}$$

$$\times \begin{pmatrix} \text{Re} \\ \text{Im} \end{pmatrix}\{\Psi_{m+2,\mathbf{R}}^*(\mathbf{r})\Psi_{m+1,\mathbf{R}}(\mathbf{r})g_{m;m+2}^{(2)<}(\mathbf{R},\omega)$$

$$+ \Psi_{m+1,\mathbf{R}}(\mathbf{r})\Psi_{m,\mathbf{R}}^*(\mathbf{r})[g_{m;m}^{(2)<}(\mathbf{R},\omega) - \Delta_{\mathbf{R}}g_{m;m}^{(0)<}(\mathbf{R},\omega)]\}.$$
(C7)

After using Eqs. (54) and (58) and performing the remaining energy integration, we can rewrite expression (C7) as

$$\mathbf{j}^{(2)}(\mathbf{r}) = \frac{e}{h}\int d^2\mathbf{R}\sum_{m=0}^{+\infty}\frac{l_B^2}{2}\left\{\left[n_F'[\xi_m(\mathbf{R})]\left[m\Delta_{\mathbf{R}}V - \frac{|\nabla_{\mathbf{R}}V|^2}{\hbar\omega_c}\right] - n_F''[\xi_m(\mathbf{R})]\frac{|\nabla_{\mathbf{R}}V|^2}{2} + \frac{|\nabla_{\mathbf{R}}V|^2}{(\hbar\omega_c)^2}\{mn_F[\xi_{m-1}(\mathbf{R})] + (m+1)n_F[\xi_{m+1}(\mathbf{R})]\right.\right.$$

$$-(2m+1)n_F[\xi_m(\mathbf{R})]\}\right]\hbar\omega_c\nabla_{\mathbf{r}}\left[\sum_{p=0}^{m}|\Psi_{p,\mathbf{R}}(\mathbf{r})|^2 - \frac{|\Psi_{m,\mathbf{R}}(\mathbf{r})|^2}{2}\right] + (m+1)\left\{[n_F[\xi_{m+2}(\mathbf{R})] + n_F[\xi_m(\mathbf{R})] - 2n_F[\xi_{m+1}(\mathbf{R})]]\right.$$

$$\times\left[\frac{\nabla_{\mathbf{R}}V(\nabla_{\mathbf{R}}V\cdot\nabla_{\mathbf{r}})}{\hbar\omega_c} - \frac{|\nabla_{\mathbf{R}}V|^2}{2\hbar\omega_c}\nabla_{\mathbf{r}}\right] + [n_F[\xi_{m+2}(\mathbf{R})] - n_F[\xi_m(\mathbf{R})]]\left[\frac{(\nabla_{\mathbf{r}}\cdot\nabla_{\mathbf{R}})\nabla_{\mathbf{R}}V}{2} - \frac{\Delta V}{4}\nabla_{\mathbf{r}}\right]\right\}\sum_{p=0}^{m+1}|\Psi_{p,\mathbf{R}}(\mathbf{r})|^2\right\} \times \hat{\mathbf{z}}.(C8)$$

c. Contribution from $g^{(3)}$

Finally, there exist second-order contributions to the current density coming from the elements of third-order Green's function $g^{(3)}$ which couple adjacent Landau levels [this contribution arises from the second term in the right-hand side of Eq. (71)]. Similar to the previous calculation, these recombine nicely with the contribution from the function $g^{(1)}$ associated with the term $k=1$ in Eq. (71). Our starting expression thus reads

$$\mathbf{j}^{(3)}(\mathbf{r}) = \frac{e\hbar}{m^*}\int\frac{d\omega}{2\pi}\int\frac{d^2\mathbf{R}}{2\pi l_B^2}\sum_{m=0}^{+\infty}\frac{l_B^2}{2}\sqrt{m}|\Psi_{m,\mathbf{R}}(\mathbf{r})|^2\begin{pmatrix}\text{Im}\\\text{Re}\end{pmatrix}[i\Delta_{\mathbf{R}}g_{m;m-1}^{(1)<}(\mathbf{R},\omega) - ig_{m;m-1}^{(3)<}(\mathbf{R},\omega)].$$
(C9)

Inserting the explicit expressions for the first- and third-order Green's functions [expressions (31) and (A6)–(A9)] and performing the integration over the energy ω, we finally find after tedious calculations,

$$\mathbf{j}^{(3)}(\mathbf{r}) = \frac{e}{h}\hat{\mathbf{z}} \times \int d^2\mathbf{R}\sum_{m=0}^{+\infty}\frac{l_B^2}{2}m|\Psi_{m,\mathbf{R}}(\mathbf{r})|^2\left\{\frac{m+1}{2}[n_F[\xi_m(\mathbf{R})] - n_F[\xi_{m-1}(\mathbf{R})]]\Delta_{\mathbf{R}}\nabla_{\mathbf{R}}V + \left[(m+2)n_F'[\xi_m(\mathbf{R})] - mn_F'[\xi_{m-1}(\mathbf{R})]\right.\right.$$

$$+\frac{2}{\hbar\omega_c}[n_F[\xi_{m-1}(\mathbf{R})] - n_F[\xi_m(\mathbf{R})]]\right]\Delta_{\mathbf{R}}V\nabla_{\mathbf{R}}V + \Delta\{[n_F[\xi_{m-1}(\mathbf{R})] - n_F[\xi_m(\mathbf{R})]]\nabla_{\mathbf{R}}V\} + \frac{1}{4\hbar\omega_c}[\Delta_{\mathbf{R}}V\nabla_{\mathbf{R}}V - \nabla_{\mathbf{R}}\{|\nabla_{\mathbf{R}}V|^2\}]$$

$$\times[4\hbar\omega_c n_F'[\xi_{m-1}(\mathbf{R})] + (m+1)[n_F[\xi_{m-1}(\mathbf{R})] - n_F[\xi_{m+1}(\mathbf{R})]]$$

$$+(m-1)[n_F[\xi_m(\mathbf{R})] - n_F[\xi_{m-2}(\mathbf{R})]]] + [(m+1)n_F[\xi_{m+1}(\mathbf{R})] - (m-1)n_F[\xi_{m-2}(\mathbf{R})] + (3m-1)n_F[\xi_{m-1}(\mathbf{R})]$$

$$-(3m+1)n_F[\xi_m(\mathbf{R})] + (\hbar\omega_c)^2[n_F''[\xi_m(\mathbf{R})] - n_F''[\xi_{m-1}(\mathbf{R})]] + 2\hbar\omega_c[n_F'[\xi_{m-1}(\mathbf{R})] - n_F'[\xi_m(\mathbf{R})]]]\frac{|\nabla_{\mathbf{R}}V|^2\nabla_{\mathbf{R}}V}{2(\hbar\omega_c)^2}\right\}.$$
(C10)

2. Semiclassical expressions for the current

The second-order contributions involve several terms according to their different possible origins. A first term comes with the expansion of the density-gradient contribution $\mathbf{j}^{(0)}$ [Eq. (72)],

$$\mathbf{j}^{(0)}(\mathbf{r}) = \frac{e}{h}\frac{l_B^2}{2}\sum_{m=0}^{+\infty}\frac{(m+1)^2}{2}\hbar\omega_c\Delta_{\mathbf{r}}\boldsymbol{\nabla}_{\mathbf{r}}[n_F(\xi_m(\mathbf{r}))]\times\hat{\mathbf{z}},\tag{C11}$$

where we have used Eq. (60). After making two integration by parts and using Eq. (60), the second-order term for the current density arising from Green's function $g^{(1)}$ [Eqs. (75) and (C6)] takes the form

$$\mathbf{j}^{(1)}(\mathbf{r}) = \frac{e}{h}\frac{l_B^2}{2}\sum_{m=0}^{+\infty}(3m+2)\Delta_{\mathbf{r}}\{n_F[\xi_m(\mathbf{r})]\boldsymbol{\nabla}_{\mathbf{r}}V\}\times\hat{\mathbf{z}}.\tag{C12}$$

Second-order terms brought by the contribution $\mathbf{j}^{(2)}$ are written as

$$
\begin{aligned}
\mathbf{j}^{(2)}(\mathbf{r}) = \frac{e}{h}\frac{l_B^2}{2}\sum_{m=0}^{+\infty}&\left\{\left(m+\frac{1}{2}\right)\hbar\omega_c\boldsymbol{\nabla}_{\mathbf{r}}\left[n_F'[\xi_m(\mathbf{r})]\left(m\Delta_{\mathbf{r}}V - \frac{|\boldsymbol{\nabla}_{\mathbf{r}}V|^2}{\hbar\omega_c}\right) - n_F''[\xi_m(\mathbf{r})]\frac{|\boldsymbol{\nabla}_{\mathbf{r}}V|^2}{2}\right]\times\hat{\mathbf{z}} + \frac{2}{\hbar\omega_c}[n_F[\xi_m(\mathbf{r})](\boldsymbol{\nabla}_{\mathbf{r}}V\cdot\boldsymbol{\nabla}_{\mathbf{r}})\boldsymbol{\nabla}_{\mathbf{r}}V\right.\\
&\left. + (\boldsymbol{\nabla}_{\mathbf{r}}\cdot\{n_F[\xi_m(\mathbf{r})]\boldsymbol{\nabla}_{\mathbf{r}}V\})\boldsymbol{\nabla}_{\mathbf{r}}V\times\hat{\mathbf{z}} + \left(m+\frac{1}{2}\right)[\Delta_{\mathbf{r}}V\boldsymbol{\nabla}_{\mathbf{r}}n_F[\xi_m(\mathbf{r})] - n_F[\xi_m(\mathbf{r})]\Delta_{\mathbf{r}}\boldsymbol{\nabla}_{\mathbf{r}}V - 2(\boldsymbol{\nabla}_{\mathbf{r}}n_F[\xi_m(\mathbf{r})]\cdot\boldsymbol{\nabla}_{\mathbf{r}})\boldsymbol{\nabla}_{\mathbf{r}}V]\times\hat{\mathbf{z}}\right\}.
\end{aligned}
\tag{C13}
$$

Finally, the terms originating from the contribution $\mathbf{j}^{(3)}$ yield the following second-order correction to the current density,

$$
\begin{aligned}
\mathbf{j}^{(3)}(\mathbf{r}) = \frac{e}{h}\frac{l_B^2}{2}\sum_{m=0}^{+\infty}\hat{\mathbf{z}}\times&\left\{(m+1)n_F'[\xi_m(\mathbf{r})][\Delta_{\mathbf{r}}V\boldsymbol{\nabla}_{\mathbf{r}}V - \boldsymbol{\nabla}_{\mathbf{r}}(|\boldsymbol{\nabla}_{\mathbf{r}}V|^2)] + \left\{\frac{2}{\hbar\omega_c}n_F[\xi_m(\mathbf{r})] - n_F'[\xi_m(\mathbf{r})]\right\}\Delta_{\mathbf{r}}V\boldsymbol{\nabla}_{\mathbf{r}}V\right.\\
&\left. + \left\{\frac{n_F'[\xi_m(\mathbf{r})]}{\hbar\omega_c} - \frac{n_F''[\xi_m(\mathbf{r})]}{2}\right\}|\boldsymbol{\nabla}_{\mathbf{r}}V|^2\boldsymbol{\nabla}_{\mathbf{r}}V - (m+1)n_F[\xi_m(\mathbf{r})]\Delta_{\mathbf{r}}\boldsymbol{\nabla}_{\mathbf{r}}V + \Delta_{\mathbf{r}}[n_F[\xi_m(\mathbf{r})]\boldsymbol{\nabla}_{\mathbf{r}}V]\right\}.
\end{aligned}
\tag{C14}
$$

[1] K. v. Klitzing, G. Dorda, and M. Pepper, Phys. Rev. Lett. **45**, 494 (1980).

[2] K. von Klitzing, Philos. Trans. R. Soc. London, Ser. A **363**, 2203 (2005).

[3] R. G. Mani, J. H. Smet, K. v. Klitzing, V. Narayanamurti, W. B. Johnson, and V. Umansky, Nature (London) **420**, 646 (2002).

[4] K. S. Novoselov, A. K. Geim, S. V. Morozov, D. Jiang, M. I. Katsnelson, I. V. Grigorieva, S. V. Dubonos, and A. A. Firsov, Nature (London) **438**, 197 (2005).

[5] P. Weitz, E. Ahlswede, J. Weis, K. von Klitzing, and K. Eberl, Physica E (Amsterdam) **6**, 247 (2000).

[6] S. Ilani, J. Martin, E. Teitelbaum, J. H. Smet, D. Mahalu, V. Umansky, and A. Yacoby, Nature (London) **427**, 328 (2004).

[7] G. A. Steele, R. C. Ashoori, L. N. Pfeiffer, and K. W. West, Phys. Rev. Lett. **95**, 136804 (2005).

[8] J. Weis, Int. J. Mod. Phys. B **21**, 1297 (2007).

[9] R. F. Kazarinov and S. Luryi, Phys. Rev. B **25**, 7626 (1982).

[10] S. A. Trugman, Phys. Rev. B **27**, 7539 (1983).

[11] S. M. Apenko and Yu. E. Lozovik, J. Phys. C **16**, L591 (1983).

[12] R. Joynt and R. E. Prange, Phys. Rev. B **29**, 3303 (1984).

[13] S. M. Apenko and Yu. E. Lozovik, J. Phys. C **17**, 3585 (1984).

[14] S. M. Apenko and Yu. E. Lozovik, J. Phys. C **18**, 1197 (1985).

[15] B. Shapiro, Phys. Rev. B **33**, 8447 (1986).

[16] *The Quantum Hall Effect*, edited by R. E. Prange and S. M. Girvin (Springer, New York, 1987).

[17] J. T. Chalker and P. D. Coddington, J. Phys. C **21**, 2665 (1988).

[18] B. Huckestein, Rev. Mod. Phys. **67**, 357 (1995).

[19] D. B. Chklovskii, B. I. Shklovskii, and L. I. Glazman, Phys. Rev. B **46**, 4026 (1992).

[20] K. Lier and R. R. Gerhardts, Phys. Rev. B **50**, 7757 (1994).

[21] R. B. Laughlin, Phys. Rev. B **23**, 5632 (1981).

[22] B. I. Halperin, Phys. Rev. B **25**, 2185 (1982).

[23] A. H. MacDonald and P. Streda, Phys. Rev. B **29**, 1616 (1984).

[24] M. Büttiker, Phys. Rev. B **38**, 9375 (1988).

[25] P. Streda, J. Phys. C **15**, L717 (1982).

[26] C. Wexler and D. J. Thouless, Phys. Rev. B **49**, 4815 (1994).

[27] C. Sohrmann and R. A. Römer, New J. Phys. **9**, 97 (2007).

[28] N. R. Cooper and J. T. Chalker, Phys. Rev. B **48**, 4530 (1993).

[29] K. Güven and R. R. Gerhardts, Phys. Rev. B **67**, 115327 (2003).

[30] A. Siddiki and R. R. Gerhardts, Phys. Rev. B **70**, 195335 (2004).

[31] I. M. Ruzin, Phys. Rev. B **47**, 15727 (1993).

[32] A. M. Dykhne and I. M. Ruzin, Phys. Rev. B **50**, 2369 (1994).

[33] S. H. Simon and B. I. Halperin, Phys. Rev. Lett. **73**, 3278 (1994).

[34] F. D. M. Haldane and K. Yang, Phys. Rev. Lett. **78**, 298 (1997).

[35] T. Champel and S. Florens, Phys. Rev. B **75**, 245326 (2007).

[36] M. R. Geller and G. Vignale, Phys. Rev. B **50**, 11714 (1994).

[37] D. B. Chklovskii, K. A. Matveev, and B. I. Shklovskii, Phys. Rev. B **47**, 12605 (1993).

[38] U. Wulf, V. Gudmundsson, and R. R. Gerhardts, Phys. Rev. B

38, 4218 (1988).

[39] H. Akera and H. Suzuura, J. Phys. Soc. Jpn. **74**, 997 (2005).

[40] K. Tsemekhman, V. Tsemekhman, C. Wexler, and D. J. Thouless, Solid State Commun. **101**, 549 (1997).

[41] I. Ruzin and S. Feng, Phys. Rev. Lett. **74**, 154 (1995).

[42] R. Ilan, N. R. Cooper, and A. Stern, Phys. Rev. B **73**, 235333 (2006).

[43] H. A. Fertig and B. I. Halperin, Phys. Rev. B **36**, 7969 (1987).

[44] B. Kramer, T. Ohtsuki, and S. Kettemann, Phys. Rep. **417**, 211 (2005).